

NSWCDD/TR-92/477

STRUCTURAL PERFORMANCE OF CANDIDATE ABLATIVES FOR UPTAKE SECTION OF VERTICAL LAUNCHING SYSTEM

BY JOHN W. POWERS
WEAPONS SYSTEMS DEPARTMENT

OCTOBER 1992

Approved for public release; distribution is unlimited.

NAVAL SURFACE WARFARE CENTER
DAHLGREN DIVISION
Dahlgren, Virginia 22448-5000

Accession For	
NTIS GRA&I	<input checked="checked" type="checkbox"/>
DTIC TAB	<input type="checkbox"/>
Unannounced	<input type="checkbox"/>
Justification	
By	
Distribution/	
Availability Codes	
Dist	Avail and/or Special
A-1	

FOREWORD

This project is part of an ongoing effort by NSWCDD to identify superior ablatives for use in the Vertical Launching System (VLS). The primary purpose of this segment of the effort is to identify relevant issues regarding the structural requirements for ablatives in the uptake section of the VLS. In doing so, the structural integrity of several ablatives being considered for the uptake are evaluated. The results of the theoretical derivations obtained in this report have been incorporated into a code called SABLAT to facilitate analysis of ablatives that may be considered in the future.

This work presented here was funded by the Systems Engineering Branch (G21) of the Missile Systems Division (G20).

Approved by:



DAVID S. MALYEVAC, Deputy Head
Weapons Systems Department

ABSTRACT

The structural performance of several candidate ablative for the uptake section of the Navy's Vertical Launching System is investigated. The uptake is modeled using a fixed-fixed beam loaded by a uniform pressure. Beam displacement field equations are solved, assuming that the ablative exhibit bimodular behavior in tension and compression. The candidate ablative are ranked according to predicted structural performance. The current uptake ablative, MXBE-350, possesses the highest factor of safety in this analysis, although all but one of the ablative considered appears to be acceptable. Additionally, the effects of erosion on the magnitudes of the peak stresses seen by the virgin ablative are analyzed by varying the thickness of the ablative in the uptake. As the thickness of the ablative decreases, the peak stresses in the ablative decrease. Finally, the effect of the stiffness of the ablative on predicted stresses in the adhesive layer is computed. As the elastic modulus of the ablative increases, the stresses in the adhesive decrease.

CONTENTS

<u>Chapter</u>		<u>Page</u>
1	OVERVIEW AND BACKGROUND	1
	1.1 INTRODUCTION	1
2	ABLATIVE MECHANICAL PROPERTIES	3
	2.1 ABLATIVES TESTED	3
	2.2 RESULTS OF MECHANICAL TESTS	4
3	ANALYSIS METHOD USED TO EVALUATE ABLATIVE STRUCTURAL PERFORMANCE.....	7
	3.1 PREVIOUS WORK TO CHARACTERIZE ABLATIVE STRUCTURAL PERFORMANCE	7
	3.2 OVERVIEW OF CURRENT ANALYSIS.....	11
	3.3 AREA MOMENT OF INERTIA	11
	3.4 BEAM DEFLECTIONS AND BENDING MOMENTS	20
	3.5 CALCULATION OF STRESSES IN BEAM	26
4	RESULTS OF ANALYSIS	29
	4.1 OVERVIEW OF RESULTS	29
	4.2 STRESS VS. STRENGTH OF CANDIDATE ABLATIVES	29
	4.3 EROSION EFFECTS.....	32
	4.4 EFFECT OF ABLATIVE STIFFNESS ON STRESS LEVELS IN ABLATIVE.....	32
5	CONCLUSIONS AND RECOMMENDATIONS.....	35
	5.1 GENERAL OBSERVATIONS.....	35
	5.2 POTENTIAL FOR BRITTLE FRACTURE	35
6	REFERENCES	39
7	NOMENCLATURE.....	41
 APPENDIXES		
A	CODE FOR CALCULATING STRENGTH OF ABLATIVES (SABLAT)	A-1
B	DEFLECTIONS AND BENDING STRESSES ON TOP SURFACE OF BEAM VS. AXIAL POSITION	B-1
C	BENDING STRESSES OF TOP SURFACE OF BEAM VS. ABLATIVE THICKNESS	C-1
D	SHEAR STRESS IN ADHESIVE LAYER VS. ABLATIVE ELASTIC MODULUS.....	D-1
DISTRIBUTION.....		(1)

ILLUSTRATIONS

Figure		Page
2-1	COORDINATE DIRECTIONS ON SHEET OF ABLATIVE	4
3-1	UPTAKE DEFLECTION PATTERNS IN (A) VERTICAL AND (B) HORIZONTAL DIRECTIONS OF VLS.....	7
3-2	BEAM CROSS-SECTION.....	8
3-3	FIXED-FIXED BEAM USED TO MODEL DEFLECTIONS IN UPTAKE	8
3-4	CROSS-SECTION OF BEAM USED TO MODEL UPTAKE RESPONSE	12
3-5	EQUIVALENT BEAM CROSS-SECTION ASSUMING POSITIVE MOMENT AND THAT NEUTRAL AXIS PASSES THROUGH STEEL.....	13
3-6	EQUIVALENT BEAM CROSS-SECTION ASSUMING POSITIVE MOMENT AND THAT NEUTRAL AXIS PASSES THROUGH ADHESIVE.....	15
3-7	EQUIVALENT BEAM CROSS-SECTION ASSUMING POSITIVE MOMENT AND THAT NEUTRAL AXIS PASSES THROUGH ABLATIVE	18
3-8	FIXED-FIXED BEAM LOADED BY UNIFORM PRESSURE WITH CONSTANT MOMENT OF INERTIA.....	20
3-9	BENDING MOMENTS AS FUNCTION OF AXIAL POSITION FOR BEAM IN FIGURE 3-8	21
3-10	FIXED-FIXED BEAM LOADED BY A UNIFORM PRESSURE WHERE VALUE OF I SHIFTS DEPENDING ON SIGN OF M	21
3-11	BEAM MODEL PRODUCED WHEN SYMMETRY IS APPLIED TO BEAM SHOWN IN FIGURE 3-10	22
3-12	STATE OF STRESS AT AN ARBITRARY POINT IN BEAM.....	28

TABLES

<u>Table</u>	<u>Page</u>
2-1 DESCRIPTION OF ABLATIVES TESTED IN THIS ROUND OF INVESTIGATION.....	3
2-2 SUMMARY OF AVAILABLE ELASTIC PROPERTIES FOR VARIOUS ABLATIVES CONSIDERED.....	5
2-3 ELASTIC MODULI AND STRENGTHS USED FOR THIS ANALYSIS	5
3-1 SECTION PROPERTIES FOR CROSS-SECTION SHOWN IN FIGURE 3-5 (ASSUMING NEUTRAL AXIS PASSES THROUGH STEEL AND POSITIVE MOMENT IS APPLIED)	13
3-2 SECTION PROPERTIES FOR CROSS-SECTION SHOWN IN FIGURE 3-6 (ASSUMING NEUTRAL AXIS PASSES THROUGH ADHESIVE AND POSITIVE MOMENT IS APPLIED)	16
3-3 SECTION PROPERTIES FOR CROSS-SECTION SHOWN IN FIGURE 3-7 (ASSUMING NEUTRAL AXIS PASSES THROUGH THE ABLATIVE AND POSITIVE MOMENT IS APPLIED)	18
4-1 PARAMETERS USED IN SECTION 4.2 ANALYSIS.....	30
4-2 PEAK DEFLECTIONS AND STRESSES PREDICTED FOR EACH ABLATIVE ...	31
4-3 ABLATIVES RANKED IN TERMS OF PREDICTED STRUCTURAL PERFORMANCE.....	31
4-4 PARAMETERS USED IN ANALYSIS OF SECTION 4.4.....	33
4-5 SUMMARY OF PREDICTED MAXIMUM AND MINIMUM SHEAR STRESSES IN ADHESIVE AT END OF BEAM.....	34
5-1 SMALL FLAW LOCATED IN ABLATIVE.....	36

CHAPTER 1

OVERVIEW AND BACKGROUND

1.1 INTRODUCTION

The purpose of the work presented here is to evaluate the structural integrity of ablatives being considered for use in the uptake section of the Vertical Launching System (VLS). It is part of an ongoing effort by Naval Surface Warfare Center (NSWCDD) and Food Machine Corporation (FMC) to identify candidate ablatives that are superior to the ablatives currently in use in the VLS. The primary goals of this effort are to identify new ablatives that have improved erosion resistance over existing ablatives, have low thermal diffusivities, are compatible with at-sea environments, and that will be structurally sound under the mechanical loads apparent in a launcher. New ablatives with these properties have the potential to increase both the life and the performance capabilities of the VLS. Further background on other aspects of this effort can be found in References 1 and 2.

The structural evaluation of the candidate ablatives entails two steps. The first step is to test the ablatives to determine their mechanical properties. Most of the ablatives considered are relatively new so that these properties were not readily available at the onset of this investigation. The mechanical properties have been determined using both 4-point bend tests and compression tests on samples of each material considered. The results of these tests are given in Chapter 2. The details of the test procedures used to obtain the mechanical properties are documented in Reference 3.

The second step in the structural evaluation consists of modeling the uptake with the ablatives in place to determine the stress levels in the ablatives. In this analysis, the uptake is modeled as a beam. This beam has fixed-fixed ends and is loaded by a uniform pressure. The ablative model used demonstrates different elastic properties in tension and compression. This corresponds to the actual behavior of the ablatives considered. The results of the analysis given here have been incorporated into a code called "SABLAT" (for Strength of Ablatives). This code is explained in more detail in Appendix A.

In the analysis that follows, the peak tensile and compressive stresses are predicted for different ablatives in the uptake. The tensile and compressive stresses are then divided by the tensile and compressive strengths of each ablative, respectively, to determine a factor of safety (F.S.). It is this F.S. that is used to rate the structural performance of each ablative. In the uptake, erosion of the ablative can be a serious problem. Thus, the sensitivity of the peak stresses in the ablative to the thickness of the ablative is also investigated. Finally, the effects of varying the stiffness of the ablative on the stresses in the adhesive are studied.

Although the model used is a rather simple representation of a very complex problem, it provides good insight into the behavior of the uptake with different ablatives attached and the effect of different variables on this behavior. A more detailed model might consist of finite elements. However, it would use a very complicated mesh and would have to be rerun each time

geometric or elastic parameters were modified. As a result, it is difficult to change parameters in the problem and to assess the effects of these parameters over a wide range of values. Thus, the much simpler beam model that is utilized in this analysis has been developed.

CHAPTER 2

ABLATIVE MECHANICAL PROPERTIES

2.1 ABLATIVES TESTED

In this round of the investigation, the structural performances of six ablative materials are evaluated. These ablative materials are listed in Table 2-1. All the ablative materials tested are made from composite materials. As a result, they tend to exhibit different elastic properties in different directions. Additionally, the materials exhibit bimodular elastic behavior such that the elastic properties are different depending on whether the part is in tension or compression.

TABLE 2-1. DESCRIPTION OF ABLATIVES TESTED IN
THIS ROUND OF INVESTIGATION

ABLATIVE	MANUFACTURER	MATRIX MATERIAL	FIBER MATERIAL	COMMENTS
MXBE-350	ICI Fiberite	Elastomer Modified Phenolic	Fiberglass	Current Ablative in Uptake of VLS
MXB-360	ICI Fiberite	Phenolic	Fiberglass	Current Ablative in Plenum of VLS
FR-1	Fiber Materials Incorporated	Fire Retardant Phenolic	Ceramic	
CD208-40	Haveg	41N Phenolic	Chopped Carbon, Glass, and Ceramic	
FM16771-F	ICI Fiberite	Phenolic	Chopped Glass Roving	
FM16771-A	American Polytherm	Phenolic	Chopped Glass Roving	

Consider the sheet of ablative shown in Figure 2-1. The three coordinate directions are ξ_1 , ξ_2 , and ξ_3 . All the ablative materials tested thus far have either a random weave or randomly oriented fibers in the 1-2 plane. Thus, the ablative materials are assumed to be isotropic in this plane. They will, however, have different properties in the ξ_3 direction.

Because of limitations on the amount of testing that could be performed, only the properties in the 1-2 plane have been determined. At any rate, little work has been performed on characterizing the behavior of composites considering both orthotropic behavior and differences in the tensile and compressive properties. Consequently, even if the general orthotropic properties of each ablative were known, an analysis involving both of these considerations would require extensive derivations and would be extremely time consuming and costly. It is believed that this would be beyond the scope of the current analysis.

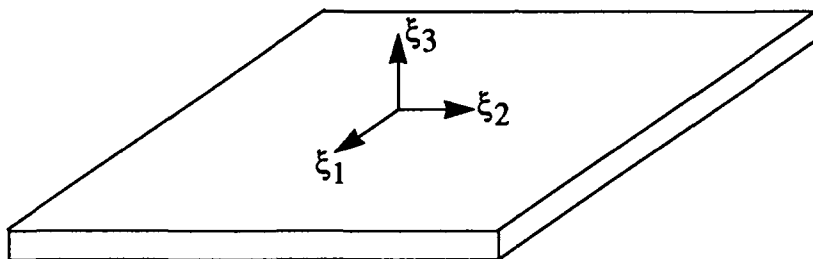


FIGURE 2-1. COORDINATE DIRECTIONS ON SHEET OF ABLATIVE

The largest loads in the ablatives will be caused by bending and occur in the 1-2 plane. The ablatives currently being considered are essentially isotropic in this plane so that orthotropic effects will only occur out of the plane and will be small. Thus, isotropic assumptions must be used in the analysis that follows. It is believed that the variances between tensile and compressive properties will influence the results much more than variances in material direction. The differences in the tensile and compressive properties have been measured and are accounted for in the analysis.

2.2 RESULTS OF MECHANICAL TESTS

Both flexural and compressive tests were performed on each ablative to determine both the tensile and compressive elastic moduli and strengths. The test procedure and complete results are documented in Reference 3. The results of these tests are summarized in Table 2-2. Additionally, elastic moduli and strengths for MXBE-350 and MXB-360 as given by Fiberite are listed in this table. In Table 2-2, E_t and E_c are the tensile and compressive moduli, respectively, and S_{ut} and S_{uc} are the tensile and compressive strengths, respectively. For the columns denoting values for E_t and E_c , the average values from all of the flexural and compressive tests performed in Reference 3 are listed. To be conservative, the minimum strengths for S_{ut} and S_{uc} from all the specimens tested in Reference 3 are listed.

Note that some discrepancies exist in the data depending on the test method and source. To account for these discrepancies, numbers will be used that yield the most conservative results. It turns out that in this analysis, the highest overall stresses are predicted when E_t and E_c are the highest (although tensile stresses are maximized when E_t is maximized and E_c is minimized while compressive stresses are maximized when E_t is minimized, and E_c is maximized). Thus, the

highest elastic modulus is used when different values are given by two sources. Additionally, when values of strength differ for materials, the minimum strength is used in the analysis. The elastic properties that will be used for this analysis are listed in Table 2-3.

TABLE 2-2. SUMMARY OF AVAILABLE ELASTIC PROPERTIES FOR VARIOUS ABLATIVES CONSIDERED

MATERIAL	TEST METHOD	E _t (Msi)	E _c (Msi)	Su _t (ksi)	Su _c (ksi)
MXBE-350	Flexural Compressive Fiberite Data	1.05	1.93	12.0	12.0
		0.90	0.82	5.0	9.5
MXB-360	Flexural Compressive Fiberite Data	3.69	6.21	23.0	31.0
		2.40	2.19	10.0	25.0
FR-1	Flexural Compressive	2.93	0.935	6.0	13.25
			0.66		
CD208-40	Flexural Compressive	1.51	3.17	4.0	8.00
			0.71		
FM16771-F	Flexural Compressive	2.21	5.83	2.5	8.00
			1.19		
FM16771-A	Flexural Compressive	6.63	1.96	17.5	15.00
			1.57		

TABLE 2-3. ELASTIC MODULI AND STRENGTHS USED FOR THIS ANALYSIS

MATERIAL	E _t (Msi)	E _c (Msi)	Su _t (ksi)	Su _c (ksi)
MXBE-350	1.05	1.93	5.0	9.5
MXB-360	3.69	6.21	10.0	25.0
FR-1	2.93	0.935	6.0	13.25
CD208-40	1.51	3.17	4.0	8.0
FM16771-F	2.21	5.83	2.5	8.0
FM16771-A	6.63	1.96	17.5	15.0

CHAPTER 3

ANALYSIS METHOD USED TO EVALUATE ABLATIVE STRUCTURAL PERFORMANCE

3.1 PREVIOUS WORK TO CHARACTERIZE ABLATIVE STRUCTURAL PERFORMANCE

Much of the work presented here is based upon a previous attempt at characterizing the structural requirements for ablative in the uptake that was recently performed by FMC (see Reference 4). FMC considered two separate cases in their analysis: one in which the ablative is rigidly bonded to the steel plate of the uptake, and one in which the adhesive bonding the ablative to the uptake is compliant. The first case, in which the ablative is assumed to be rigidly bonded to the uptake, gives the most conservative results. Consequently, only this case is described here.

In their analysis, FMC uses results from hydrostatic tests that were performed on the uptake section to determine the deflection patterns in the horizontal and vertical directions under an internal pressure of 45 psi (see Reference 5). These deflection patterns are shown in Figure 3-1. From these patterns, FMC inferred that the uptake could be modeled as a fixed-fixed beam in the vertical and in the horizontal directions. Between these two cases, FMC found that the horizontal deflection pattern provides the worst-case situation.

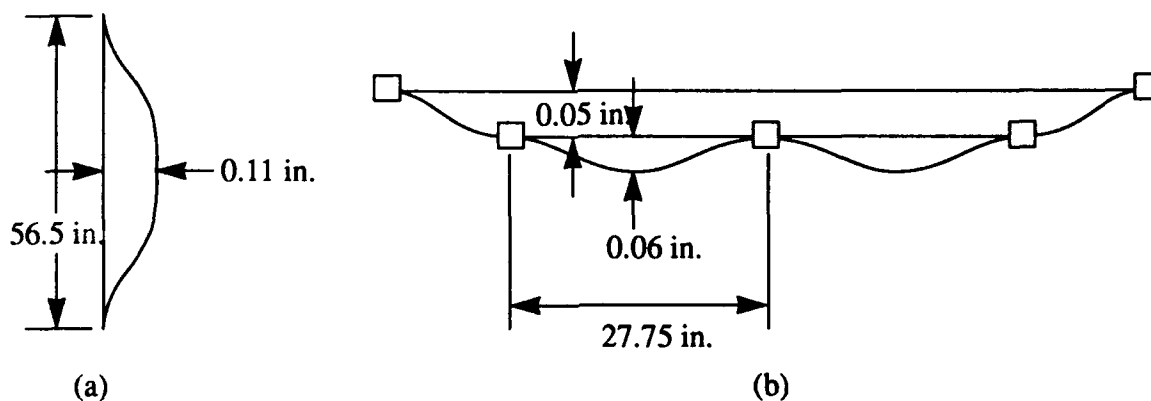


FIGURE 3-1. UPTAKE DEFLECTION PATTERNS IN (A) VERTICAL AND
(B) HORIZONTAL DIRECTIONS OF VLS

The horizontal beam cross-section used by FMC is shown in Figure 3-2. It consists of an 8.54 in. wide section of the uptake. The ablative is rigidly bonded to the steel and is assumed to be 0.38 in. thick. The moment of inertia for this cross-section is calculated using a Young's modulus of 30 Msi for the steel. In their analysis, three representative elastic moduli are considered by FMC: 1.0, 2.5, and 5.0 Msi.

Since the ablative has a different modulus of elasticity than the steel, an effective width must be used for the ablative to determine the moment of inertia. This width is given by the relation

$$w_{eff} = w \left(\frac{E_a}{E_s} \right) \quad (3-1)$$

where w is the original width of the ablative (8.54 in.), E_a is the elastic modulus of the ablative, and E_s is the elastic modulus of the steel (30 Msi). Using w_{eff} , a new equivalent cross-section made entirely of steel is obtained. (The concept of an equivalent cross-section will be explained in more detail in the next section.)

Based on the horizontal deflection pattern shown in Figure 3-1b, the beam is assumed to have clamped-clamped boundary conditions and a span of 27.75 in. The beam is also loaded by a uniform pressure q_0 . FMC's model is shown in Figure 3-3. In this analysis, the deflections of the beam used by FMC are fixed so that they match the deflection pattern shown in Figure 3-1b. As a result, a maximum deflection of 0.06 in. at the center of the beam is used for all ablatives considered.

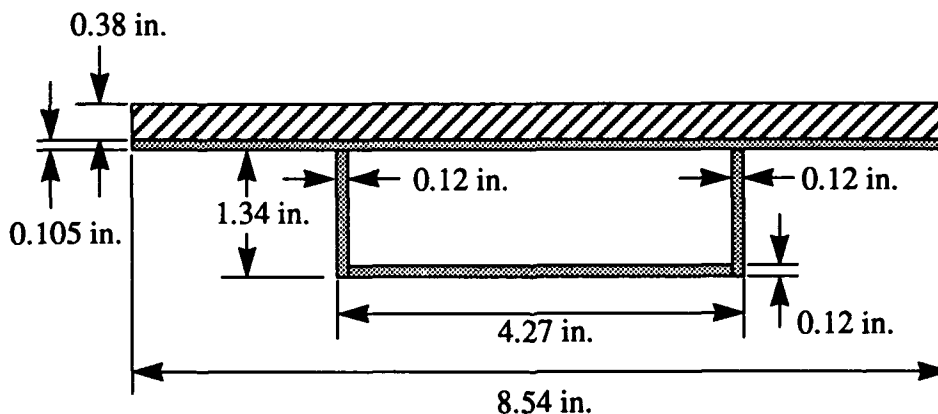


FIGURE 3-2. BEAM CROSS-SECTION

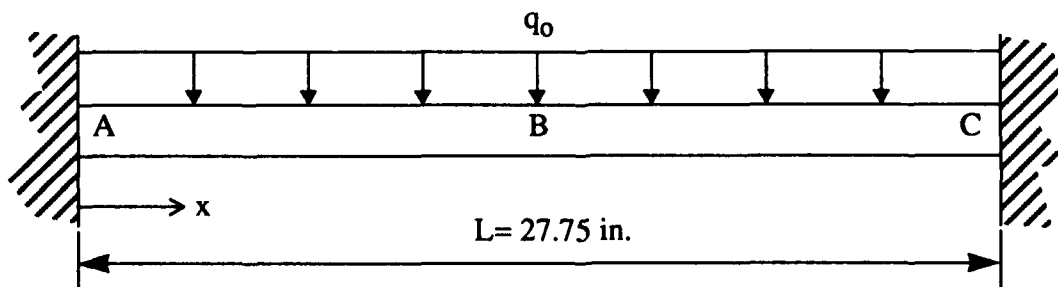


FIGURE 3-3. FIXED-FIXED BEAM USED TO MODEL DEFLECTIONS IN UPTAKE

For a fixed-fixed beam with a uniform cross-section and moment of inertia, the deflection at the center of the beam is given by the relation

$$y(x = L/2) = \frac{q_o L^4}{384 \times E_s I} \quad (3-2)$$

where L is the length of the beam and I is the moment of inertia of the beam. The bending moment at the ends of the beam are

$$M_a = \frac{-q_o L^2}{12} \quad (3-3)$$

and the moment at the center is given by

$$M_b = \frac{-q_o L^2}{24} \quad (3-4)$$

The bending stress in the ablative is found using the relation

$$\sigma_b = \frac{Mc}{I} \left(\frac{E_a}{E_s} \right) \quad (3-5)$$

where c is the distance from the neutral axis of the beam to the point in the beam where stresses are desired. The ratio (Ea/Es) is needed to convert from stresses in the equivalent steel section to stresses in the ablative section.

Equation 3-2 can be rewritten in terms of M_a such that

$$y(x = L/2) = \frac{L^2 M_a}{32 E_s} \quad (3-6)$$

Note that in Equation 3-6, the pressure q_o has dropped out and no longer has an effect on the results. At this point, the maximum deflection is fixed at 0.06 in. to match the deflections obtained in the hydrostatic test. Making this substitution into Equation 3-6 and solving for the moment gives

$$M_a = 32 \times (0.06) \frac{E_s I}{L^2} \quad (3-7)$$

The bending stress at the ends of the beam is obtained by substituting Equation 3-7 into Equation 3-5. Doing so yields

$$\sigma_b(x=0) = \frac{1.92cE_a}{L^2} \quad (3-8)$$

Stresses at the center of the beam are found in the same manner except that Equation 3-4 is now substituted into Equation 3-2. Again, the peak deflection is fixed at 0.06 in. This results in a compressive stress at the center of the beam of

$$\sigma_b(x=L/2) = -\frac{\sigma_b(x=0)}{2} \quad (3-9)$$

FMC plotted Equation 3-8 as a function of the tensile elastic modulus of the ablative for $E_a = 1.0, 2.5, \text{ and } 5.0 \text{ Msi}$ and drew a line through the three resultant points to get the relation

$$\sigma_b(x=0) = (1822 \times 10^{-6}) E_{a_t} + 430 \quad (3-10)$$

In this equation, E_{a_t} refers to the ablative's tensile modulus. The tensile modulus of the ablative must be such that the Equation 3-10 does not exceed the tensile strength of the ablative. Or,

$$S_{ut} > (1822 \times 10^{-6}) E_{a_t} + 430 \quad (3-11)$$

Similarly, plotting the results of Equation 3-9 for different compressive elastic moduli results in the condition

$$S_{uc} > (911 \times 10^{-6}) E_{a_c} + 215 \quad (3-12)$$

Equations 3-11 and 3-12 are the criteria given by FMC to define the structural requirements of the ablatives in the VLS.

One downfall of this approach is that the deflections are assumed to be fixed at 0.06 in. The problem with this is that this deflection was obtained with MXBE-350 in the uptake. If another ablative with a different elastic modulus were to be put in place of the MXBE-350, the deflections would change. For example, if the uptake were to be hydrotested with a stiffer ablative attached,

one would expect the peak deflection to be less than 0.06 in. However, in the model derived above, the peak deflection is fixed at 0.06 in. Forcing this stiffer ablative to comply with this deflection results in artificially high stresses being predicted in the ablative. Thus, the model above will tend to overpredict the stresses in an ablative that is stiffer than MXBE-350 and underpredict the stresses in an ablative that is less stiff.

Additionally, if one were to back out the pressure (q_0) from the preceding equations, one would find that the pressures would have to increase with stiffer ablatives to force the ablative to conform to the 0.06 in. peak deflection. Thus, in this model, the pressures in the uptake vary depending on the elastic modulus of the ablative. In the actual uptake, however, the pressure is the independent parameter, and the deflections depend upon both the magnitude of this pressure (which should be constant no matter which ablative is used) and the stiffness of the ablative.

3.2 OVERVIEW OF CURRENT ANALYSIS

The present analysis will attempt to refine and improve upon FMC's model, although an attempt will be made to keep the analysis simple. For this reason, the simple beam model developed by FMC will be modified and used in this analysis. The major modifications in the model will be:

- 1) pressure will be fixed and deflections will be allowed to vary
- 2) variables will be included to allow the adhesive layer between the ablative and the steel to be modeled once its properties are known
- 3) the beam deflection equations will be rederived so that they take into account the differences in the elastic moduli of the ablative in tension and in compression.

3.3 AREA MOMENT OF INERTIA

The same general beam cross-section that was used by FMC will be used here. The primary difference is that a section will be added for the adhesive layer bonding the ablative to the steel. The cross-section used, then, is shown in Figure 3-4. In the calculations that follow, it is assumed that the bending moment produces much higher forces within the beam than shear forces. A positive bending moment is defined such that it produces compressive stresses on the top surface and tensile stresses on the bottom surface of the beam. Also, in the beam model developed in the next section, it will be assumed that the beam has no externally applied axial forces. Thus, the bending moment alone is used to determine whether a point in the cross-section is in tension or compression.

It might be helpful to note that here and in the derivations that follow, the subscript c will denote a property when the material is in compression, and the subscript t will denote a property when the material is in tension. Also note that the suffix a denotes that the property is associated with the ablative, and the suffix g denotes that the property is associated with the adhesive (or glue) layer.

In this cross-section, it is assumed that the ablative and the adhesive can have different properties in tension and compression. As a result, the moment of inertia will change depending

on whether there is a positive or a negative moment. Under a positive moment, everything above the neutral axis will be in compression and everything below the neutral axis will be in tension. Under a negative moment, this situation is reversed.

For now, assume the neutral axis passes through the steel. Under a positive moment, both the ablative and the adhesive layers will be in compression so that their compressive elastic moduli are used. To calculate the moment of inertia of the beam, an equivalent cross-section will be developed. (See also any basic strength of materials text, such as References 6 and 7 for a more indepth explanation of this methodology.) Since the elastic modulus of steel remains constant at 30.0 Msi in both tension and compression, the equivalent cross-section will be made entirely of steel. To obtain this equivalent steel cross-section, the widths of the adhesive and ablative layers are adjusted so that the new cross-section has the same stiffness as the original beam. The width of the ablative layer in this equivalent beam is

$$wa_c = w \cdot \left(\frac{Ea_c}{E_s} \right) \quad (3-13)$$

where w is the original width of the ablative and Ea_c is the elastic modulus of the ablative in compression. The effective width of the adhesive layer is

$$wg_c = w \cdot \left(\frac{Eg_c}{E_s} \right) \quad (3-14)$$

where Eg_c is the elastic modulus of the adhesive in compression. The equivalent cross-section obtained is shown in Figure 3-5.

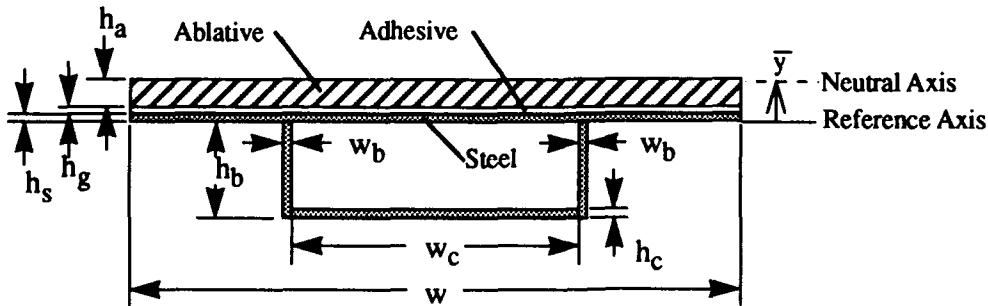


FIGURE 3-4. CROSS-SECTION OF BEAM USED TO MODEL UPTAKE RESPONSE

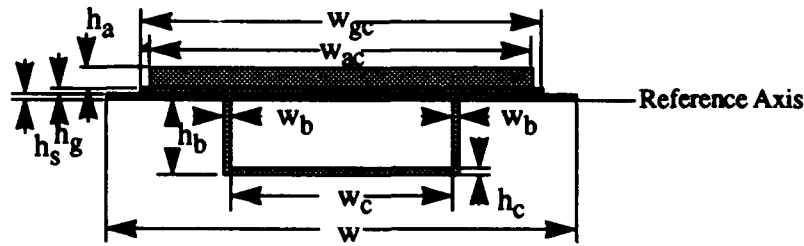


FIGURE 3-5. EQUIVALENT BEAM CROSS-SECTION ASSUMING POSITIVE MOMENT AND THAT NEUTRAL AXIS PASSES THROUGH STEEL

The moment of inertia for the equivalent cross-section shown in Figure 3-5 is calculated using the values shown in Table 3-1. In this table, A_r is the area of the section, y is the distance from the centroid of the section to the reference axis, M_y is the first moment of the cross-section, and I_y is the second moment. I_{cg} is the moment of inertia about the centroid of the section.

TABLE 3-1. SECTION PROPERTIES FOR CROSS-SECTION SHOWN IN FIGURE 3-5
(ASSUMING NEUTRAL AXIS PASSES THROUGH STEEL AND POSITIVE MOMENT IS APPLIED)

SECTION	A_r	y	$M_y = A_r * y$	$I_y = A_r * y^2$	I_{cg}
Ablative	$h_a * w_{ac}$	$h_s + h_g + h_a/2$	$(h_a * w_{ac}) * (h_s + h_g + h_a/2)$	$(h_a * w_{ac}) * (h_s + h_g + h_a/2)^2$	$w_{ac} * h_a^3/12$
Adhesive	$h_g * w_{gc}$	$h_s + h_g/2$	$(h_g * w_{gc}) * (h_s + h_g/2)$	$(h_g * w_{gc}) * (h_s + h_g/2)^2$	$w_{gc} * h_g^3/12$
Steel Plate	$h_s * w$	$h_s/2$	$h_s^2 * w/2$	$h_s^3 * w/4$	$w * h_s^3/12$
B	$2 * h_b * w_b$	$-h_b/2$	$-h_b^2 * w_b/2$	$h_b^3 * w_b/2$	$w_b * h_b^3/6$
C	$h_c * w_c$	$(h_c/2 - h_b)$	$(h_c * w_c) * (h_c/2 - h_b)$	$(h_c * w_c) * (h_c/2 - h_b)^2$	$w_c * h_c^3/12$

The location of the neutral axis for the entire cross-section is found using the relation

$$\bar{y} = \frac{\sum M_y}{\sum A_r} \quad (3-15)$$

and the moment of inertia for the entire cross-section is found using

$$I = \sum Iy + \sum Icg - (\bar{y})^2 \sum Ar \quad (3-16)$$

In Equations 3-15 and 3-16, the sum refers to the sum of all the values in that particular column.

Note that in order for the assumption that the neutral axis passes through the steel to be valid, \bar{y} must be less than h_s . If \bar{y} is greater than h_s , then it must be assumed that the neutral axis passes through the adhesive layer. In this case, under a positive moment, both the part of the adhesive above the neutral axis and the entire ablative are in compression. Thus, their respective compressive moduli must be used. The portion of the adhesive layer that lies below the neutral axis is in tension, and the tensile modulus of the adhesive will be used for it.

As was done before, an equivalent steel beam cross-section is developed. The equivalent width of the ablative is

$$wa_c = w \cdot \left(\frac{Ea_c}{E_s} \right) \quad (3-17)$$

The equivalent width of the adhesive in compression is

$$wg_c = w \cdot \left(\frac{Eg_c}{E_s} \right) \quad (3-18)$$

and the equivalent width of the adhesive in tension (below the neutral axis) is

$$wg_t = w \cdot \left(\frac{Eg_t}{E_s} \right) \quad (3-19)$$

In Equation 3-19, Eg_t refers to the tensile elastic modulus of the adhesive.

The equivalent cross-section obtained is shown in Figure 3-6. In this figure, note that hg_t and hg_c are the thicknesses of the adhesive layer in tension and compression, respectively, and are as of yet unknown. The sectional properties used to calculate \bar{y} and I for the cross-section of Figure 3-5 are listed in Table 3-2.

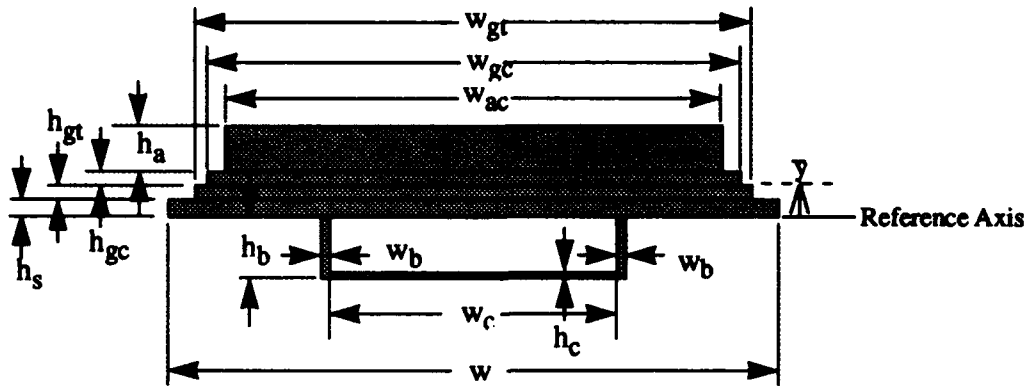


FIGURE 3-6. EQUIVALENT BEAM CROSS-SECTION ASSUMING POSITIVE MOMENT AND THAT NEUTRAL AXIS PASSES THROUGH ADHESIVE

From Figure 3-6, it can be seen that

$$\bar{y} = h_s + h_{gt} \quad (3-20)$$

Substituting this expression into Equation 3-15 gives

$$\bar{y} = h_s + h_{gt} = \frac{\sum My}{\sum Ar} \quad (3-21)$$

where $\sum My$ and $\sum Ar$ are now obtained from Table 3-2. Also note from Figure 3-6 that

$$h_{gc} = h_g - h_{gt} \quad (3-22)$$

TABLE 3-2. SECTION PROPERTIES FOR CROSS-SECTION SHOWN IN FIGURE 3-6
(ASSUMING NEUTRAL AXIS PASSES THROUGH ADHESIVE AND
POSITIVE MOMENT IS APPLIED)

SECTION	Ar	y	My=Ar*y	Iy=Ar*y ²	Icg
Ablative	ha*wa _c	hs+hg+ha/ 2	(ha*wa _c)* (hs+hg+ha/2)	(ha*wa _c)* (hs+hg+ha/2) ²	wa _c *ha ³ /12
Adhesive (above neutral axis)	hg _c *wg _c	hs+hg _t + hg _c /2	(hg _c *wg _c)* (hs+hg _t +hg _c /2)	(hg _c *wg _c)* (hs+hg _t + hg _c /2) ²	wg _c *hg _c ³ / 12
Adhesive (below neutral axis)	hgt*wg _t	hs+hg _t /2	(hgt*wg _t)* (hs+ hg _t /2)	(hgt*wg _t)* (hs+ hg _t /2) ²	wg _t *hg _t ³ /12
Steel Plate	hs*w	hs/2	hs ² *w/2	hs ³ *w/4	w*hs ³ /12
B	2*hb*wb	-hb/2	-hb ² /wb	hb ³ *wb/2	wb*hb ³ /6
C	hc*wc	(hc/2-hb)	(hc*wc)* (hc/2-hb)	(hc*wc)* (ha/2-hb) ²	wc*hc ³ /12

Upon substituting the results from Table 3-2 and Equation 3-22 into Equation 3-21, hg_t can be solved for. Doing so gives

$$hg_t = \frac{-C_2 \pm \sqrt{C_2^2 - 4C_1C_3}}{2C_1} \quad (3-23)$$

where

$$C_1 = \frac{wg_t}{2} - \frac{wg_c}{2} \quad (3-24a)$$

$$C_2 = hg \cdot wg_c + ha \times wa_c + hs \times w + 2(hb \cdot wb) + hc \cdot wc \quad (3-24b)$$

and

$$C_3 = \frac{hs^2w}{2} + 2hb \times hs \times wb + hc \times hs \times wc -$$

$$\frac{hg^2 \times wg_c}{2} - ha \times hg \times wa_c - \frac{ha^2 \times wa_c}{2} +$$

$$hb^2 wb - \frac{hc^2 wc}{2} + hb \times hc \times wc \quad (3-24c)$$

The value of hg_t is the positive root of Equation 3-23. At this point, \bar{y} can be found from Equation 3-20 and hg_c can be found from Equation 3-22. If \bar{y} is between hs and $(hs + hg)$, then the assumption that \bar{y} passes through the ablative is correct, and the moment of inertia can be calculated using Equation 3-16.

If \bar{y} is greater than $(hs + hg)$, the neutral axis passes through the ablative. When this is the case, a new equivalent steel cross-section must be used. With the neutral axis in the ablative, a positive moment will cause the ablative above the neutral axis to be in compression and the ablative below the neutral axis to be in tension. The entire adhesive layer will be in tension. In this situation, the effective width of the ablative section above the neutral axis is

$$wa_c = w \left(\frac{Ea_c}{Es} \right) \quad (3-25)$$

and the effective width for the ablative below the neutral axis is

$$wa_t = w \left(\frac{Ea_t}{Es} \right) \quad (3-26)$$

In Equation 3-26, Ea_t is the tensile elastic modulus of the ablative. The effective width of the adhesive is

$$wg_t = w \left(\frac{Eg_t}{Es} \right) \quad (3-27)$$

The new effective steel cross-section then, is shown in Figure 3-7, and the sectional properties are listed in Table 3-3.

In Figure 3-7 and Table 3-3, ha_t and ha_c are unknown since \bar{y} has not been found yet. However, from Figure 3-7, it is apparent that

$$ha_c = ha - ha_t \quad (3-28)$$

and

$$\bar{y} = h_s + h_g + h_{a_t} \quad (3-29)$$

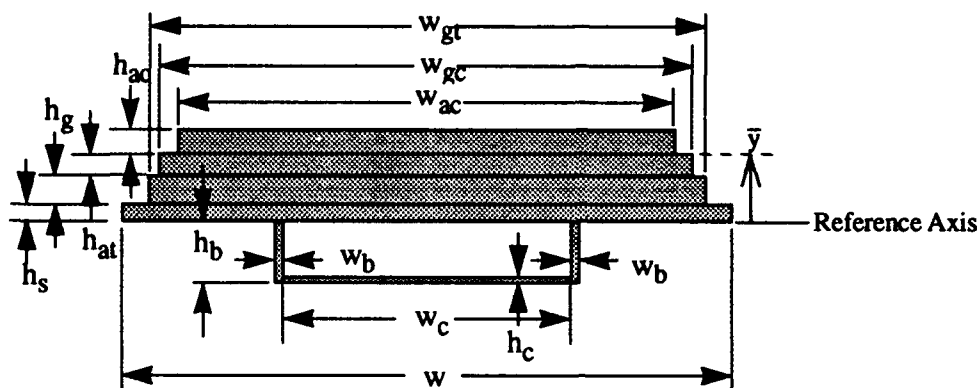


FIGURE 3-7. EQUIVALENT BEAM CROSS-SECTION ASSUMING POSITIVE MOMENT AND THAT NEUTRAL AXIS PASSES THROUGH ABLATIVE

TABLE 3-3. SECTION PROPERTIES FOR CROSS-SECTION SHOWN IN FIGURE 3-7
(ASSUMING NEUTRAL AXIS PASSES THROUGH THE ABLATIVE AND POSITIVE MOMENT IS APPLIED)

SECTION	A_r	y	$M_y = A_r \cdot y$	$I_y = A_r \cdot y^2$	I_{cg}
Ablative (above neutral axis)	$h_{a_c} \cdot w_{a_c}$	$h_s + h_g + h_{a_t} + h_{a_c}/2$	$(h_{a_c} \cdot w_{a_c}) \cdot (h_s + h_g + h_{a_t} + h_{a_c}/2)$	$(h_{a_c} \cdot w_{a_c}) \cdot (h_s + h_g + h_{a_t} + h_{a_c}/2)^2$	$w_{a_c} \cdot h_{a_c}^3/12$
Ablative (below neutral axis)	$h_{a_t} \cdot w_{a_t}$	$h_s + h_g + h_{a_t}/2$	$(h_{a_t} \cdot w_{a_t}) \cdot (h_s + h_g + h_{a_t}/2)$	$(h_{a_t} \cdot w_{a_t}) \cdot (h_s + h_g + h_{a_t}/2)^2$	$w_{a_t} \cdot h_{a_t}^3/12$
Adhesive	$h_g \cdot w_{g_t}$	$h_s + h_g/2$	$(h_g \cdot w_{g_t}) \cdot (h_s + h_g/2)$	$(h_g \cdot w_{g_t}) \cdot (h_s + h_g/2)^2$	$w_{g_t} \cdot h_g^3/12$
Steel Plate	$h_s \cdot w$	$h_s/2$	$h_s^2 \cdot w/2$	$h_s^3 \cdot w/4$	$w \cdot h_s^3/12$
B	$2 \cdot h_b \cdot w_b$	$-h_b/2$	$-h_b^2 \cdot w_b$	$h_b^3 \cdot w_b/2$	$w_b \cdot h_b^3/6$
C	$h_c \cdot w_c$	$(h_c/2 - h_b)$	$(h_c \cdot w_c) \cdot (h_c/2 - h_b)$	$(h_c \cdot w_c) \cdot (h_c/2 - h_b)^2$	$w_c \cdot h_c^3/12$

Substituting Equation 3-29 into Equation 3-15 gives

$$\bar{y} = hs + hg + ha_t = \frac{\sum My}{\sum Ar} \quad (3-30)$$

Table 3-3 is used to find $\sum My$ and $\sum Ar$. Substituting these summations and Equation 3-28 into Equation 3-30, ha_t is found to be the positive root of

$$ha_t = \frac{-C_5 \pm \sqrt{C_5^2 - 4C_4C_6}}{2C_4} \quad (3-31)$$

with

$$C_4 = \frac{wa_t}{2} - \frac{wa_c}{2} \quad (3-32a)$$

$$C_5 = ha \times wa_c + hg \times wg_t + hs \times w + 2hb \times wb + hc \times wb \quad (3-32b)$$

and

$$\begin{aligned} C_6 = & \frac{hs^2 \times w}{2} + 2hb \times hs \times wb + hc \times hs \times wc + \frac{hg^2 \times wg}{2} + \\ & hg \times hs \times w + 2hb \times hg \times wb + hc \times hg \times wc + hb^2 wb - \\ & \frac{hc^2 wc}{2} + hb \times hc \times wc - \frac{ha^2 wa_c}{2} \end{aligned} \quad (3-32c)$$

Once ha_t has been determined, ha_c can be found from Equation 3-28, and \bar{y} can be found from Equation 3-29. Finally, Equation 3-16 is used with the section properties in Table 3-3 to find I.

The previous calculations to determine the moment of inertia for the beam under a bending moment all assume that a positive moment is being applied. In the case where a negative moment is applied, the same results are used except that the values for tension and compression are reversed. For example, if the neutral axis passes through the steel and a negative moment is applied, the adhesive and ablative layers will be in tension. Thus, the effective widths in the transformed beam will be

$$wg_t = w \cdot \left(\frac{Eg_t}{Es} \right) \quad (3-33)$$

and

$$wa_t = w \cdot \left(\frac{Ea_t}{Es} \right) \quad (3-34)$$

for the adhesive and ablative layers, respectively. Then, in Figure 3-5 and Table 3-1, wg_t is substituted for wg_c and wa_t is substituted for wa_c .

3.4 BEAM DEFLECTIONS AND BENDING MOMENTS

As was done in FMC's analysis, the uptake is modeled as a fixed-fixed beam loaded by a uniform pressure. One shortcoming of FMC's model, however, is that it assumes that the beam has a constant moment of inertia. Consider the fixed-fixed beam shown in Figure 3-8. It is loaded by a uniform pressure and has a constant elastic modulus and moment of inertia. For this type of beam, it is well known that the bending moment as a function of axial position is

$$M(x) = \frac{q_0}{12} [6Lx - L^2 - 6x^2] \quad (3-35)$$

Equation 3-35 is plotted in Figure 3-9.

Note that in Figure 3-9 the bending moment shifts from negative to positive and back to negative again. In Section 3-3, it was noted that the moment of inertia of the beam changes depending on whether the applied moment is positive or negative (since the elastic moduli of the ablative and adhesive layers are assumed to change depending on whether the part is in tension or compression). Thus, when M changes sign, one would expect that the value of the moment of inertia changes. As a result, the solution given by Equation 3-35 is no longer completely valid since it was obtained assuming that the moment of inertia is constant.

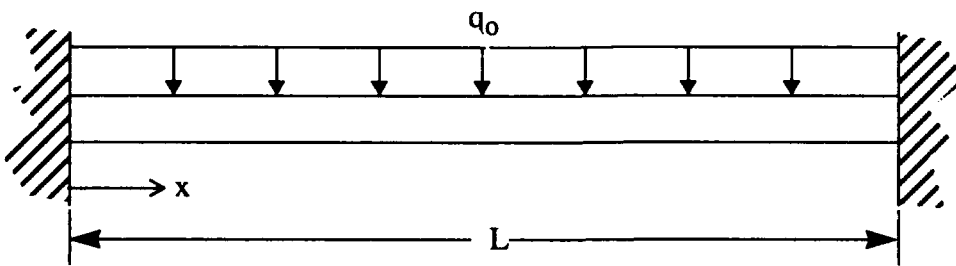


FIGURE 3-8. FIXED-FIXED BEAM LOADED BY UNIFORM PRESSURE WITH CONSTANT MOMENT OF INERTIA

Given this information, a new fixed-fixed beam can be derived that reflects these changes. This new beam is shown in Figure 3-10. Note that at both ends of the beam where the moment is negative (and the top surface of the ablative is in tension), the moment of inertia is given as I_1 .

Between A and B, where the moment shifts to a positive value, the moment of inertia shifts to I_2 (corresponding to the top surface of the beam being in compression).

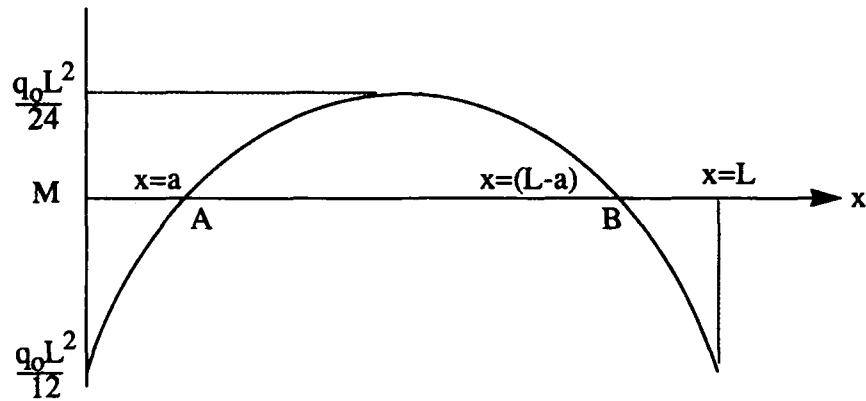


FIGURE 3-9. BENDING MOMENTS AS FUNCTION OF AXIAL POSITION FOR BEAM IN FIGURE 3-8

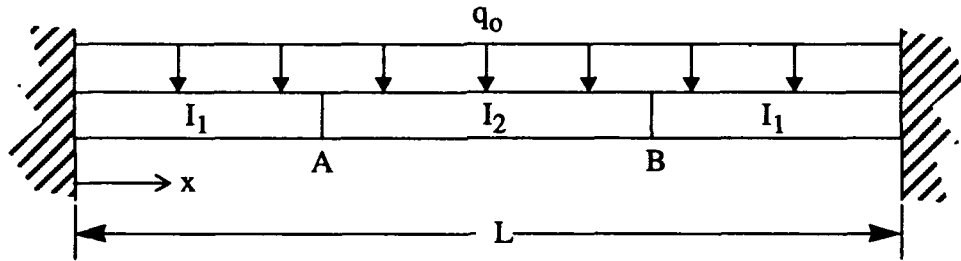


FIGURE 3-10. FIXED-FIXED BEAM LOADED BY A UNIFORM PRESSURE WHERE VALUE OF I SHIFTS DEPENDING ON SIGN OF M

To account for these shifts in I , the differential equation for the displacement fields in a beam must be solved. This equation is given by

$$\frac{d^2}{dx^2} \left[EI(x) \frac{d^2 y}{dx^2} \right] = q(x) \quad (3-36)$$

In this relation, y is the deflection of the beam, E is the elastic modulus of the beam (since the transformed beam cross-section derived in Section 3.2 is made of steel, $E = E_s = 30.0$ Msi), and $q(x)$ is the applied pressure. Since both E and $q(x)$ are constant for the beam shown in Figure 3-10, Equation 3-36 may be rewritten as

$$\frac{d^2}{dx^2} \left[I(x) \frac{d^2 y}{dx^2} \right] = \frac{q_0}{E_s} \quad (3-37)$$

Equation 3-37 must now be solved in terms of the beam's boundary conditions. However, before this is done, it is helpful to note that the beam's deflection will be symmetric about its midspan ($x = L/2$). Utilizing this symmetry produces the simplified model shown in Figure 3-11. In the beam shown in Figure 3-11, note that the moment of inertia shifts from I_1 to I_2 at $x = a$. This is the point at which the moment shifts from negative to positive and is as of yet undetermined. Also note that in the following solution, the deflections of the beam will be solved for in two sections. The first section has the moment of inertia I_1 and the second section has the moment of inertia I_2 . The boundary conditions at the point where I_1 and I_2 meet ($x = a$) will be set equal for both sections.

The four boundary conditions at the ends of the beam shown in Figure 3-11 are

- (i) $y_1(x=0) = 0$
- (ii) $y_1'(x=0) = 0$
- (iii) $y_2'(x=L/2) = 0$
- (iv) $E_s I_2 y_2'''(x=L/2) = 0$

Note that boundary condition (i) denotes zero deflection at the left end, boundary conditions (ii) and (iii) denote zero slope at either end, and condition (iv) denotes zero shear at the right end. The values for y_1 refer to deflections in the section of the beam with I_1 and the values for y_2 refer to deflections in the section with I_2 . The symbol ' refers to the derivative with respect to x .

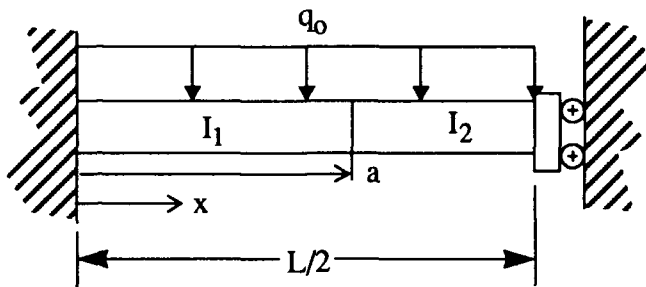


FIGURE 3-11. BEAM MODEL PRODUCED WHEN SYMMETRY IS APPLIED TO BEAM SHOWN IN FIGURE 3-10

Four more boundary conditions may be obtained at the interface of the I_1 and I_2 sections on the beam. They are

- (v) $y_1(x=a) = y_2(x=a)$
- (vi) $y_1'(x=a) = y_2'(x=a)$
- (vii) $E_s I_1 y_1''(x=a) = E_s I_2 y_2''(x=a)$
- (viii) $E_s I_1 y_1'''(x=a) = E_s I_2 y_2'''(x=a)$

These boundary conditions simply state that the deflections, slopes, moments, and shears of both beam sections must be equal at $x = a$.

Now consider the solution of Equation 3-37 for $x < a$. The equation can be written as

$$\frac{d^4 y}{dx^4} = \frac{q_0}{Es \times I1} \quad (3-38)$$

The homogeneous solution of this differential equation is

$$y1_h = Ax^3 + Bx^2 + Cx + D \quad (3-39a)$$

and the particular solution is

$$y1_p = \frac{K}{I1} x^4 \quad (3-39b)$$

where

$$K = \frac{q_0}{24Es} \quad (3-40)$$

The total solution is the sum of the homogeneous and particular solutions:

$$y1 = Ax^3 + Bx^2 + Cx + D + \frac{K}{I1} x^4 \quad (3-41a)$$

$$y1' = 3Ax^2 + 2Bx + C + \frac{4K}{I1} x^3 \quad (3-41b)$$

$$y1'' = 6Ax + 2B + \frac{12K}{I1} x^2 \quad (3-41c)$$

$$y1''' = 6A + \frac{24K}{I1} x \quad (3-41d)$$

The coefficients A, B, C, and D must be solved for using the boundary conditions.

Next consider the solution of Equation 3-37 for $a < x < L/2$. The equation can be rewritten as

$$\frac{d^4 y}{dx^4} = \frac{q_0}{Es \times I2} \quad (3-42)$$

Solving this in the same manner as Equation 3-38 yields

$$y_2 = Fx^3 + Gx^2 + Hx + J + \frac{K}{I_2}x^4 \quad (3-43a)$$

$$y_2' = 3Fx^2 + 2Gx + H + \frac{4K}{I_2}x^3 \quad (3-43b)$$

$$y_2'' = 6Fx + 2G + \frac{12K}{I_2}x^2 \quad (3-43c)$$

$$y_2''' = 6F + \frac{24K}{I_2}x \quad (3-43d)$$

At this point there are 9 unknowns that must be determined: A, B, C, D, F, G, H, J, and a.

Shear Conditions

Applying boundary condition (iv) stating that there is no shear at the right end of the beam to Equation 3-43d gives

$$F = -\frac{2KL}{I_2} \quad (3-44)$$

Applying boundary condition (viii) to Equations 3-41d and 3-43d yields

$$A = -\frac{2KL}{I_1} \quad (3-45)$$

Moment Condition

Applying boundary condition (vii) describing moments at the interface between the two beam sections to Equations 3-41c and 3-43c gives

$$B = \left(\frac{I_2}{I_1}\right) \times G \quad (3-46)$$

Slope Conditions

From boundary condition (ii) and Equation 3-41b, the coefficient C is found to be

$$C = 0 \quad (3-47)$$

The coefficient H is found in terms of G by applying boundary condition (iii) to Equation 3-43b and is given by

$$H = \frac{KL^3}{I_2} - GL \quad (3-48)$$

Now, matching the slopes of the two beam sections at $x=a$ (from boundary condition (vi)), one obtains

$$G = \left[2a - 2a \left(\frac{I_2}{I_1} \right) - L \right]^{-1} \times \left[-\frac{6KLa^2}{I_1} + \frac{4Ka^3}{I_1} + \frac{6KLa^2}{I_2} - \frac{KL^3}{I_2} - \frac{4Ka^3}{I_2} \right] \quad (3-49)$$

Deflection Conditions

From boundary condition (i) and Equation 3-41a,

$$D = 0 \quad (3-50)$$

Matching the deflections at $x=a$ (boundary condition (v)), Equations 3-41a and 3-43a give

$$J = 2KLa^3 \left(\frac{1}{I_2} - \frac{1}{I_1} \right) + Ga^2 \left(\frac{I_2}{I_1} - 1 \right) - a \left(\frac{kL^3}{I_2} - GL \right) + Ka^4 \left(\frac{1}{I_1} - \frac{1}{I_2} \right) \quad (3-51)$$

At this point, the only variable left to find is a . The way this problem is set up, $x=a$ when the moment goes to zero. Or,

$$M(x=a) = 0$$

$$Es \cdot I_1 \cdot y_1''(x=a) = 0$$

$$6Aa + 2B + \frac{12Ka^2}{I_1} = 0 \quad (3-52)$$

Substituting the expressions for A, B, and G into Equation 3-52 yields

$$Na^3 + Pa^2 + Qa + R = 0 \quad (3-53)$$

where these coefficients are defined by

$$N = 8 \left(1 - \frac{I_2}{I_1} \right)$$

$$P = 6L \left(\frac{I_2}{I_1} \right) - 12L$$

$$Q = 6L^2$$

and

$$R = -L^3$$

In Equation 3-53, a can either be solved for numerically along the length of the beam or it can be solved using methods described in Reference 8.

Once a is known, all the other coefficients can be found so that the deflections, slopes, moments, and shears are known.

3.5 CALCULATION OF STRESSES IN BEAM

The bending stress in the transformed beam's cross-section is determined using the familiar relation

$$\sigma_b(x) = \frac{M(x)c}{I} \quad (3-54)$$

where c is the distance from the neutral axis of the transformed beam to the point of interest in the beam. Note that in the above expression, the appropriate I (I_1 or I_2) must be used depending on whether $x < a$ or $a < x < L/2$.

This equation, however, is only valid for the section of the actual beam that is made from steel. To obtain the stresses in the ablative and adhesive sections, this relation must be multiplied by the ratio of the elastic modulus of the ablative or adhesive divided by the elastic modulus for steel (E_a/E_s or E_g/E_s). If the area of interest is in compression, E_{a_c} and E_{g_c} are used. If it is in tension, E_{a_t} and E_{g_t} are used. For simplicity, the subscripts c and t will be left off here. Thus, the bending stress in the adhesive is

$$\sigma_b(x) = \frac{M(x)c}{I} \left(\frac{E_g}{E_s} \right) \quad (3-55)$$

and the bending stress in the ablative is

$$\sigma_b(x) = \frac{M(x)c}{I} \left(\frac{E_a}{E_s} \right) \quad (3-56)$$

The value of shear stresses in the beam can also be calculated. However, since the out-of-plane properties of the ablatives are not known, the values obtained from these equations are only approximate. In the steel sections of the beam, shear stresses are calculated using the relation

$$\tau(x) = \frac{V(x) \cdot A_s \cdot \bar{z}}{I \cdot t} \quad (3-57)$$

In this expression, t is the width of the transformed section, A_s is the area of the transformed beam above the point being analyzed, and \bar{z} is the distance from the centroid of A_s to the neutral axis of the beam.

As done in the calculation of bending stresses, this relation is multiplied by the ratio of the elastic moduli to obtain shear stresses in the actual beam. The shear stress in the adhesive, then, is

$$\tau(x) = \frac{V(x) \cdot A_s \cdot \bar{z}}{I \cdot t} \left(\frac{E_g}{E_s} \right) \quad (3-58)$$

and the shear stress in the ablative is

$$\tau(x) = \frac{V(x) \cdot A_s \cdot \bar{z}}{I \cdot t} \left(\frac{E_a}{E_s} \right) \quad (3-59)$$

If the material is assumed to be essentially isotropic, the state of stress at any given point is composed of both bending and shear stresses as shown in Figure 3-12. The principal stresses can be calculated using Mohr's circle. Doing so yields

$$\sigma_1 = \frac{\sigma_b}{2} + \sqrt{\left(\frac{\sigma_b}{2}\right)^2 + \tau^2} \quad (3-60a)$$

$$\sigma_2 = \frac{\sigma_b}{2} - \sqrt{\left(\frac{\sigma_b}{2}\right)^2 + \tau^2} \quad (3-60b)$$

Similarly, the principal shear stress is obtained as

$$\tau_{max} = \sqrt{\left(\frac{\sigma_b}{2}\right)^2 + \tau^2} \quad (3-61)$$

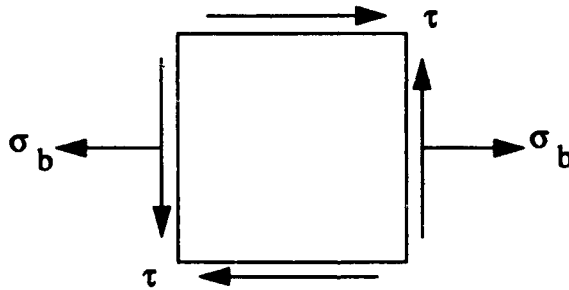


FIGURE 3-12. STATE OF STRESS AT AN ARBITRARY POINT IN BEAM

An approximate equivalent uniaxial stress can be found using the von Mises theory. This stress is given as

$$\sigma_e = \sqrt{\sigma_1^2 + \sigma_2^2 - \sigma_1 \sigma_2} \quad (3-62)$$

Failure in the beam is predicted when this equivalent stress exceeds the strength of the beam, or when

$$\sigma_e \geq \frac{Su}{F.S.} \quad (3-63)$$

In Equation 3-63, S_u is the failure strength of the beam (either S_{ut} or S_{uc} in the ablative), and F.S. is the factor of safety desired.

CHAPTER 4

RESULTS OF ANALYSIS

4.1 OVERVIEW OF RESULTS

Three general cases are analyzed in this section. The first looks at the stresses and strengths of each of the candidate ablatives. The ablatives are then ranked according to predicted structural performance. The second general case examines the effects of erosion on the structural performance of the ablatives. In doing so, the thickness of the ablative layer is varied from 0.38 in. to 0.00 in., and the effect of this variance on stresses seen by the ablative are plotted. The third set of calculations involves determining the effect of the stiffness of the ablative on the stresses seen in the adhesive. This is accomplished by assuming an adhesive thickness and varying the elastic modulus of the ablative. Note that all calculations have been made using virgin ablative properties. Thus, it has been assumed that the char layer will be thin enough so that it will not significantly affect the mechanical properties of the ablative.

In this analysis, an attempt has been made to correlate the results with the hydrostatic test data obtained by FMC. In their test, and as reported by FMC in Reference 4, a peak deflection at 45 psi of 0.06 in. was observed with a 0.38 in. thick layer of MXBE-350 in the uptake. If this pressure is applied to the beam model developed in the last section and the properties for MXBE-350 from Table 3-3 are used, a deflection of only 0.028 in. is observed. (Note that since the beam is assumed to be 8.54 in. wide, $q_0 = 45.0 \text{ lbf/in}^2 \times 8.54 \text{ in} = 384.3 \text{ lbf/in.}$) This small deflection is likely due to the fact that a simplified beam model is used to model a much more complicated structure. Since the deflections are much smaller in the beam model than were seen in the hydrotest, it is reasonable to assume that the calculated stresses in the ablative will be smaller than the actual stresses seen in the hydrotest. To correct this problem, an equivalent pressure is used in this analysis. This equivalent pressure is determined by varying q_0 until the maximum deflection of the beam with MXBE-350 is 0.06 in. This occurs when $q_0 = 824.25 \text{ lbf/in}$ (or, with an effective pressure of 96.52 lbf/in^2). This effective pressure is used for all the calculations in the analysis.

4.2 STRESS VS. STRENGTH OF CANDIDATE ABLATIVES

To predict the response of each of the candidate ablatives to the structural loads induced in the uptake of the VLS, the code SABLAT is used (see Appendix A). The fixed parameters used in each case are listed in Table 4-1. The material properties used for each ablative are listed in Table 3-3. Additionally, since the properties of the adhesive are undefined at this point, its thickness has been set at 0.00 in. It might be useful to note that in each of the cases studied, the neutral axis passes through the steel (i.e., \bar{y} is always less than h_s). As a result, the ablative is either entirely in tension or entirely in compression, depending on the sign of the bending moment.

Plots of deflections and bending stresses at the top surface of the ablative for uptake sections made from each of the candidate ablatives are plotted as functions of axial position along the beam in Appendix B. In each case, the peak tensile stress occurs at the ends of the beam ($x=0.00$ in., 27.75 in.) and the peak deflection and compressive stress occur at the midspan ($x=13.875$ in.). Note that when the bending moment changes from positive to negative, the ablative goes from tension to compression. (The point at which this happens is found using Equation 3-53.) When the bending moment switches sign, the moment of inertia of the beam changes, and the stresses in the ablative are computed using the ratio E_a/E_s instead of E_a/E_s . Thus, the shape of curve describing the bending stresses changes between these sections of the beam.

TABLE 4-1. PARAMETERS USED IN SECTION 4.2 ANALYSIS

VARIABLE	DESCRIPTION	VALUE
E_s	elastic modulus of steel	30.0 Msi
h_a	thickness of ablative	0.38 in
h_b	height of sides of C-channel	4.34 in
h_c	thickness of end of C-channel	0.12 in
h_g	thickness of adhesive	0.00 in
h_s	thickness of steel plate	0.105 in
L	length of beam	27.75 in
q_o	pressure	824.25 lbf/in.
w	width of beam	8.54 in
w_b	width of sides of C-channel	0.12 in
w_c	width of end of C-channel	4.03 in

All peak stresses occur on the top surface of the ablative where the distance from the neutral axis is maximized. The maximum deflections and peak stresses are listed for each of the candidate ablatives in Table 4-2. F.S.'s have also been calculated for each ablative in tension and compression. In tension, the F.S. is computed by dividing the ablative's tensile strength by the peak tensile stress. The F.S. in compression is computed by dividing the ablative's ultimate compressive strength by the peak compressive stress.

TABLE 4-2. PEAK DEFLECTIONS AND STRESSES PREDICTED FOR EACH ABLATIVE

ABLATIVE	PEAK DEFLECTION (IN.)	MAX. TENSILE STRESS (KSI)	TENSILE F.S.	MAX. COMPRESSIVE STRESS (KSI)	COMPRESSIVE F.S.
MXBE-350	0.0600	2.40	2.09	-2.06	4.62
MXB-360	0.0496	6.28	1.59	-4.60	5.43
FR-1	0.0576	5.62	1.07	-1.04	12.76
CD208-40	0.0568	3.23	1.24	-3.01	2.65
FM16771-F	0.0523	4.30	0.58	-4.56	1.75
FM16771-A	0.0506	9.55	1.83	-1.86	8.08

At this point, it might be helpful to note that the maximum allowable design pressure for the lower uptake section of the VLS is 45 psi. For a missile flyout, a F.S. of 1.43 is required so that the peak pressure in the uptake must not exceed 31 psi. For a restrained firing, a F.S. of 1.15 is required so that the peak pressure in the uptake must not exceed 38 psi. In the calculations presented here, the uptake deflections and pressures are based upon a hydrostatic test at 45 psi (see Section 4.1). Thus, the 1.43 and 1.15 factors of safety have already been accounted for in these calculations. The factors of safety listed in Table 4-2, then, are factors of safety above these 1.43 and 1.15 limits.

In Table 4-2, the minimum factors of safety occur when the materials are in tension. Note that FM16771-F has a tensile F.S. of less than 1.0, so it is predicted to fail. The ablatives are ranked according to predicted structural performance in Table 4-3.

TABLE 4-3. ABLATIVES RANKED IN TERMS OF PREDICTED STRUCTURAL PERFORMANCE

RANK	ABLATIVE	F.S.
1	MXBE-350	2.09
2	FM16771-A	1.83
3	MXB-360	1.59
4	CD208-40	1.24
5	FR-1	1.07
FAILED	FM16771-F	0.58

Of the ablatives currently under consideration, MXBE-350 (the current uptake ablative) shows the highest F.S. Thus, from a purely structural standpoint, it is the superior ablative. However, each of the other ablatives considered, with the exception of FM16771-F, appears to be acceptable.

4.3 EROSION EFFECTS

The effect of erosion on the stress levels experienced by the ablatives is investigated here. This is accomplished by varying the thickness of the ablative and plotting its peak tensile and compressive stresses. This procedure, then, assumes that the erosion is uniform and does not account for stress concentrations that may develop as a result of localized erosion. It also assumes that the char layer is thin and will not significantly degrade the structural performance of the ablative. In computing these stresses, the ratio of c/I , or the section modulus, becomes important (remember that c is the distance of the point of interest in the cross-section from the neutral axis and I is the moment of inertia). As seen in Section 3.5, the magnitudes of the bending stresses are proportional to this ratio. If c is the distance to the outer surface of the ablative, then as the thickness of the ablative decreases, both the value of c and I decrease. Depending on the relative magnitudes of these decreases, the stress in the ablative can either increase or decrease.

The parameters used in these calculations are the same as those listed in Table 4-1, except that the thickness of the ablative is varied from 0.00 to 0.38 in. The maximum bending stress (at $x=0$) and the maximum compressive stress (at $x=L/2=13.875$ in.) for each ablative is plotted in Appendix C as their thicknesses decrease from 0.38 to 0.00 in. Note that in nearly every case, the F.S. increases as the ablative thickness decreases. The exception is shown in Figure C-4 of Appendix C. For MXB-360, the F.S. decreases slightly as the ablative thickness decreases at the center of the beam. However, this decrease is so small that the stresses are essentially constant. Thus, uniform erosion does not appear to have a serious detrimental effect on the structural performance of any of the ablatives.

4.4 EFFECT OF ABLATIVE STIFFNESS ON STRESS LEVELS IN ADHESIVE

A potential concern in selecting a new ablative for the uptake is that if too stiff of an ablative were to be used, it could *pop* off. To assess whether this is a valid concern, the stresses in the adhesive layer are computed as a function of ablative stiffness. For simplicity, the elastic modulus of both the ablative and the adhesive are assumed to be the same in tension and compression. According to WS20174, the adhesive used in the VLS is subjected to a lap shear test on a 0.005 to 0.01 in. thick sample of the adhesive (see Reference 9). It is conceivable, however, that this thickness varies in the actual VLS. Thus, two thicknesses are assumed for the adhesive: 0.01 and 0.05 in. Since the elastic modulus of the adhesive (E_g) is unknown, cases are considered in which E_g is set at 0.5, 1.0, 5.0, and 10.0 Msi. The parameters used for the cases studied here are listed in Table 4-4.

TABLE 4-4. PARAMETERS USED IN ANALYSIS OF SECTION 4.4

VARIABLE	DESCRIPTION	VALUE
Es	elastic modulus of steel	30.0 Msi
ha	thickness of ablative	0.38 in.
hb	height of sides of C-channel	1.34 in.
hc	thickness of end of C-channel	0.12 in.
hg	thickness of adhesive	0.01 and 0.05 in.
hs	thickness of steel plate	0.105 in.
L	length of beam	27.75 in.
qo	pressure	824.25 lbf/in.
w	width of beam	8.54 in.
wb	width of sides of C-channel	0.12 in.
wc	width of end of C-channel	4.03 in.

In order to obtain a wide range of values, the ablative elastic modulus E_a is varied from 0 to 30 Msi. The principal shear stresses in the adhesive (from Equation 3-61) have been calculated at the ends of the beam where they are maximized. These stresses are plotted in Appendix D. A summary of the cases considered and the shear stresses is given in Table 4-5. Note that in Table 4-5, τ_{\max} is the maximum shear stress occurring through the range of ablative elastic moduli and τ_{\min} is the minimum shear stress. Next to each value of τ , the elastic modulus of the ablative at which the shear stress is predicted is listed. Remember that h_g and E_g refer to the thickness and the elastic modulus of the adhesive layer, respectively.

From the plots in Appendix D, note that τ_{\max} always occurs when E_a is minimized ($E_a = 0.0$ Msi), and τ_{\min} occurs when E_a is largest ($E_a = 30$ Msi, for the range of values considered). Increasing the elastic modulus of the ablative can significantly reduce the stress levels seen in the adhesive. Thus, there does not appear to be much danger of the ablative coming loose because it is too stiff.

TABLE 4-5. SUMMARY OF PREDICTED MAXIMUM AND MINIMUM SHEAR STRESSES IN ADHESIVE AT END OF BEAM

CASE	hg (in.)	Eg (Msi)	τ_{max} (ksi)/ Ea (Msi)	τ_{min} (ksi)/ Ea (Msi)
1	0.01	0.5	0.417/ 0.0	0.029/ 30.0
2	0.05	0.5	0.443/ 0.0	0.031/ 30.0
3	0.01	1.0	0.832/ 0.0	0.057/ 30.0
4	0.05	1.0	0.878/ 0.0	0.063/ 30.0
5	0.01	5.0	4.11/ 0.0	0.286/ 30.0
6	0.05	5.0	4.13/ 0.0	0.311/ 30.0
7	0.01	10.0	8.09/ 0.0	0.570/ 30.0
8	0.05	10.0	7.70/ 0.0	0.616/ 30.0

CHAPTER 5

CONCLUSIONS AND RECOMMENDATIONS

5.1 GENERAL OBSERVATIONS

A model has been developed to evaluate and rank the structural performance of several candidate ablatives for use in the uptake in the VLS. In addition, parameter studies were made to determine the effects of erosion on the stress levels in the ablative and determine the effect of ablative stiffness on the stresses in the adhesive layer. Based upon this analysis, the following observations can be made:

- 1) All but one of the ablatives considered met the criteria set forth in this report. However, one likely source of error in this analysis is in the data obtained from the flexural tests. Both the elastic moduli and the strengths obtained from the flexural tests appear to be higher than expected. The procedure used to extract the elastic properties from these tests was very involved and subject to many assumptions. It is strongly recommended that tensile tests be made on each of the materials considered to directly obtain accurate tensile properties. The analysis in Section 4.2 should then be redone using the results from the tensile and compressive tests to accurately characterize and rank the behavior of the ablatives.
- 2) Assuming uniform erosion, as the ablative erodes, the peak stresses in the ablative are either essentially constant or are reduced.
- 3) Stiffer ablatives reduce the stresses in the adhesive. There does not appear to be much chance of the ablative coming loose because it is too stiff.
- 4) It is important to note that in determining whether a candidate ablative will be suitable for the VLS, it is not so much the flexibility of the ablative that is important; rather, it is the ratio of the strength of the ablative to the predicted maximum stress in the ablative. In fact, as seen in Section 4.4, it may even be desirable to have a stiff ablative. Thus, in the evaluation of the candidate ablatives, the *flexibility* requirement previously set forth (i.e., the new ablative was to be as or more flexible than current ablatives) is not suitable. This requirement has the potential to mistakenly classify as *unacceptable* ablatives that would in fact be structurally acceptable in the uptake of the VLS.

5.2 POTENTIAL FOR BRITTLE FRACTURE

One issue not yet resolved is that of brittle fracture. The susceptibility of these ablatives to brittle fracture can not be fully determined without a complete fracture mechanics analysis. However, as a first-round approximation, consider the following analysis:

In linear elastic fracture mechanics, brittle fracture is predicted to occur when

$$K_I > K_{IC} \quad (5-1)$$

In this expression, K_I is the stress intensity factor and is a function of stress, crack size, and part geometry. K_{IC} is the plane strain fracture toughness and is a material property that can be determined using test methods described in ASTM D5045 (see Reference 10). Additionally, the object being analyzed is assumed to be loaded under plane strain conditions. If it is not, Equation 5.1 will yield conservative results.

For the parameters considered in this analysis, it turns out that the neutral axis always passes through the steel section of the beam. This means that at the center of the beam (the I2 region in Section 3.4) the ablative will be entirely in compression and at the ends (the I1 region in Section 3.4) the entire ablative will be in tension. Cracks will not propagate under pure compression, so the I2 region of the beam is not considered to be in danger of brittle fracture. The worst condition, then, will occur at the points in which the tensile stresses are the highest, or at the ends of the beam ($x=0$).

Consider the case in which a small semi-elliptical crack of length $2d$ and depth b is located in the top of the ablative at $x=0$. This is shown in Figure 5-1. It is assumed to be loaded by a uniform tensile stress of σ_b (i.e., assume variations in tensile stress caused by the bending moment are small at this scale). Also assume that the length of the crack is much greater than its depth, such as might be caused by a long, thin scratch. Using elastic theory (see for example Reference 11), it can be shown that with this geometry and loading

$$K_I = 1.12\sigma_b \cdot (\pi b)^{1/2} \quad (5-2)$$

Now, go back to Section 4.2 and, to be conservative, consider the material where the highest tensile stress is observed at the end of the beam. For FM16771-A, a peak tensile stress of 9.55 ksi is predicted. As an example, assume that a 0.10 in. deep flaw exists in the material. (This flaw would already be 25 percent through the ablative.) Then, using Equations 5-1 and 5-2 a fracture K_{IC} of 6.0 ksi*in^{1/2} would be required to keep the crack from becoming unstable and propagating through the material. For smaller initial flaw sizes, this number would go down.

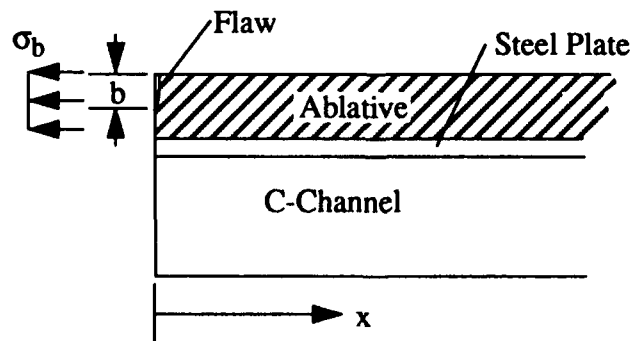


FIGURE 5-1. SMALL FLAW LOCATED IN ABLATIVE

For plane strain conditions to exist, the thickness of the ablative h_a must be such that

$$h_a \leq \left(\frac{K_{IC}}{S_u} \right)^2 \quad (5-3)$$

Taking $h_a = 0.38$ in., $K_{IC} = 6.0$, and $S_u = 17.5$ (from Table 2-3), it can be seen that this condition is satisfied. (Note that typically, the yield strength of the material is used instead of the ultimate strength. Since these materials do not demonstrate definite yield points, the ultimate strength is used for this rough analysis.)

Although the required fracture toughness is very small, it is conceivable that some of the ablatives tested could have fracture toughnesses below this. For instance, some ceramic composites have fracture toughnesses below $5.0 \text{ ksi} \cdot \text{in}^{1/2}$ (see Reference 12). Compare this with, for example, 4340 steel that can have K_{IC} 's ranging from approximately 40 to $100 \text{ ksi} \cdot \text{in}^{1/2}$, depending on the heat treatment (see Reference 13). Although this is just a quick, rough analysis, it does demonstrate that a better understanding of the toughness of the ablative is needed before this mode of failure can be completely dismissed.

5.3 RECOMMENDATIONS

Based upon the observations noted above, the following recommendations are made:

- 1) In the future, conduct three tests on candidate ablatives to determine mechanical properties:
 - (i) Tensile Test
 - (ii) Compressive Test
 - (iii) Plane Strain Fracture Toughness Test (using ASTM D5045)
- 2) Before a candidate ablative is deemed as structurally acceptable for the uptake, it must meet two strength criteria:
 - (i) The peak tensile and compressive stresses must not exceed the ultimate strengths of the ablative (i.e., using procedure explained in Chapter 3 and SABLAT code).
 - (ii) Instead of the flexibility requirement previously set forth, use fracture mechanics methods to determine the potential for brittle fracture of the ablatives.
- 3) In the future, the effect of thermal stresses in the ablatives needs to be examined. Thermal stresses produced in the ablatives will be superimposed with the mechanical stresses. Then, the sum of these stresses (mechanical and thermal) needs to be compared against the ablative strengths.

- 4) The extent to which the mechanical properties are degraded by the char that develops on the surface the ablative needs to be evaluated. In this analysis, it has been assumed that this char has only a very small effect. This assumption needs to be verified.

It must be noted that based upon the analysis in the previous section, it does not appear that there is a high probability that the materials will fail due to brittle fracture (the required K_{IC} for the example calculation is fairly small). Consequently, plane strain fracture toughness testing does not necessarily have to be performed on all of the ablatives screened. However, once the field of candidate ablatives has been narrowed down to just a few, plane strain fracture toughness tests need to be conducted to ensure that K_{IC} is within acceptable limits. If an ablative in the uptake were to fail in a brittle manner, the failure would be sudden and catastrophic. Thus, it is important that this mode of failure be understood before a new ablative is chosen.

CHAPTER 6

REFERENCES

1. Koo, J.H.; Lin S.; Kneer, M.J.; and Boyer, C.T., "Performance of High Temperature Composite Ablatives under a Hostile Environment," *37th International SAMPE Symposium and Exhibition*, Vol. 37, Anaheim, CA, March 1992.
2. Boyer, C.T., Talmy, I.G., Haught, D.A., Duffy, J.V., and Koo, J.H., "Evaluation of Fiber-Reinforced Composite Ablators Exposed to a Solid Rocket Motor Exhaust," presented at the AIAA/SAE/ASME/ASEE 28th Joint Propulsion Conference and Exhibit (as Paper AIAA-92-3510), Nashville, TN, 6-8 July 1992.
3. Deloach, K.M.; Blackmon, C.M.; and Knight, R.D., *A Method for Measuring Ablator Compressive Properties*, NSWCDD/TR-92/221, Naval Surface Warfare Center, Dahlgren, VA, in publication.
4. Glaser, J.C., "Ablative Structural Characterization," TI F1007-051, *Applied Mechanics*, Naval Systems Division, FMC Corporation, 1991.
5. "Test Description and Summary, Upper Uptake Destructive Hydrotests," VLS SM-2 Block IV Integration, FMC Corporation Naval Systems Division E.C. 1334, June 1, 1990.
6. Beer, F. B. and Johnston, E. R., *Mechanics of Materials*, McGraw-Hill, 1981.
7. Timoshenko, S., *Strength of Materials*, Part I, Elementary Theory and Problems, D. Van Nostrand Co., 1958.
8. Beyer, W.H., *CRC Standard Mathematical Tables*, 28th Edition, CRC Press Inc., 1981.
9. *Process Specification for Bonding with Structural Epoxy Adhesive*, Naval Sea Systems Command WS20174, 1982.
10. "Standard Methods for Plane-Strain Fracture Toughness and Strain Energy Release Rate of Plastic Materials," ASTM D5045, *1991 Annual Book of ASTM Standards*, 1991.
11. Ewalds, H.L. and Wanhill, R.J.H., *Fracture Mechanics*, Edward Arnold Ltd., 1986.
12. Becher, P.F. and Tiegs, T.N., "Whisker Reinforced Ceramics," Vol. 1, *Composites, Engineered Materials Handbook*, ASM International, 1987.
13. Philip, T.V. and McCaffery, T.J., "Ultrahigh Strength Steels," Vol. 1, *Metals Handbook*, 10th Ed., ASM International, 1990.

NOMENCLATURE

a = axial position in beam at which moment switches from negative to positive (in.)
 A = coefficient in solution of beam displacement fields
 A_r = area (in.²)
 A_s = area of beam above point of interest in calculation of shear stress (in.²)
 b = depth of crack (in.)
 B = coefficient in solution of beam displacement fields
 c = distance from point of interest to neutral axis (in.)
 C = coefficient in solution of beam displacement fields
 D = coefficient in solution of beam displacement fields
 d = length of crack (in.)
 E_s = elastic modulus of steel (Msi)
 E_a = elastic modulus of ablative (a subscript t denotes that it is the modulus in tension and a subscript c denotes that it is the modulus in compression) (Msi)
 E_g = elastic modulus of adhesive (a subscript t denotes that it is the modulus in tension and a subscript c denotes that it is the modulus in compression) (Msi)
 F = coefficient in solution of beam displacement fields
 G = coefficient in solution of beam displacement fields
 h_a = total thickness of ablative (in.)
 h_{a_c} = thickness of ablative section that's in compression (in.)
 h_{a_t} = thickness of ablative section that's in tension (in.)
 h_b = height of walls of C-channel (in.)
 h_c = thickness of base of C-channel (in.)
 h_g = total thickness of adhesive layer (in.)
 h_{g_c} = thickness of adhesive layer that is in compression (in.)
 h_{g_t} = thickness of adhesive layer that is in tension (in.)
 h_s = thickness of steel section (in.)
 H = coefficient in solution of beam displacement fields
 I = area moment of inertia (in.⁴)
 I_{cg} = moment of inertia about the centroid of a subsection of the beam (in.⁴)
 I_y = second moment (in.⁴)

I_1 = moment of inertia of beam section 1 (with a negative moment applied) (in.⁴)
 I_2 = moment of inertia of beam section 2 (with a positive moment applied) (in.⁴)
 J = coefficient in solution of beam displacement fields
 K_I = stress intensity factor (ksi*in.^{1/2})
 K_{IC} = mode I plane strain fracture toughness (ksi*in.^{1/2})
 L = length of the beam (in.)
 q_0 = pressure acting on the beam (lbf/in.)
 M_a = moment at the ends of a fixed-fixed beam (lbf*in.)
 M_b = moment at the center of a fixed-fixed beam (lbf*in.)
 M_y = first moment of the cross section (in.³)
 S_{uc} = ultimate compressive strength (ksi)
 S_{ut} = ultimate tensile strength (ksi)
 t = width of transformed section in calculation of shear stress (in.)
 V = shear (lbf)
 w = width of beam (in.)
 w_a = effective width of ablative section (a subscript t denotes that it is the effective width in tension and a subscript c denotes that it is the effective width in compression) (in.)
 w_b = width of walls of C-channel (in)
 w_c = width of base of C-channel (in)
 w_{eff} = effective width of section (in)
 w_g = effective width of adhesive (or glue) section (a subscript t denotes that it is the effective width in tension and a subscript c denotes that it is the effective width in compression) (in.)
 x = axial position along beam (in.)
 y = vertical deflection of beam (in.)
 \bar{y} = location of the neutral axis with respect to the reference axis (in.)
 y_1 = deflection of beam section with I_1 (in.)
 y_2 = deflection of beam section with I_2 (in.)
 \bar{z} = distance from centroid of A_s to neutral axis of beam (in.)
 σ_b = bending stress (psi)
 τ = shear stress (psi)

APPENDIX A
CODE FOR CALCULATING STRENGTH
OF ABLATIVES (SABLAT)

A Fortran code has been written incorporating the results of Chapter 3 of this report. The loading and material properties are input into the code and the peak tensile and compressive stresses are output. The tensile and compressive factors of safety are also calculated. A sample of the input prompts from the code are listed below:

SABLAT- Structural Analysis Code for the Ablative
in the Uptake of the VLS

Input the Tensile Modulus of the Ablative (Msi):
3.69
Input the Compressive Modulus of the Ablative:
6.21
Input the thickness of the ablative (in):
(recommended thickness= 0.38 in)
0.38
Input the tensile strength of the ablative (ksi):
10.0
Input the compressive strength of the ablative (ksi):
25.0
Is the adhesive layer to be included in this run?(y/n)
n
Input the pressure acting on the beam (lbf/in):
(recommended pressure= 824.25 lbf/in)
824.25
Input the length of the beam (in):
(recommended length= 27.75 in)
27.75

The output file generated by SABLAT, osablat, for these inputs is listed below

FIXED-FIXED BEAM LOADING AND LENGTH

Pressure= 824.2500 lbf/in

Length= 27.7500 in

STEEL SECTION PROPERTIES

Elastic Modulus of Steel= 30000000.00psi

Thickness of Steel Plate=0.1050 in

Width of Steel Plate=8.5400 in

C-Channel Sidewalls: Height= 1.3400 in

Width =0.1200 in

C-Channel Endwall: Height= 0.1200 in
Width =4.0300 in

ABLATIVE LAYER PROPERTIES

Tensile Modulus of Ablative= 3690000.00psi
Compressive Modulus of Ablative= 6210000.00psi
Ablative Thickness=0.3800 in
Effective Ablative Width (Compression)=1.7678in
Effective Ablative Width (tension)=1.0504in

PEAK STRESS RESULTS:

Max. Ablative Bending Stress at Ends= 6.28126 ksi
Ultimate Tensile Strength= 10.00000 ksi
Factor of Safety= 1.59204

Max. Ablative Compressive Stress at Center= -4.60355ksi
Ultimate Compressive Strength= -25.00000ksi
Factor of Safety= 5.43059

Additionally, a file "obeam" is generated that lists deflections, slopes, moments, and shears as a function of axial position along the length of the beam. The output file "ostress" outputs bending stresses on the top and bottom surfaces of the ablative and the shear and von Mises stresses along the bottom surface of the ablative.

The source code for SABLAT is listed as follows:

```
c 6/3/92- Code to calculate moments of inertia, deflections, and
c stresses in the ablative in the VLS uptake. A beam model is
c used to model the uptake.
```

```
implicit none
c Input Variables for mofi
real eat, eac, egt, egc, ha, hg, es, width
real hs, wc, hc, wb, hb
c Output Variables from mofi
real ybarp, ybarn, a, zbarn, zbarp
c Input Variables for cbeam
real mofin, mofip, length, qo
real deflect(500),dwdx(500),moment(500)
real shear(500),posit(500)
integer nsteps, i
c Variables Used to Calculate Stress
real bstress(500), ctop, cbottom, inertia,sut,suc
real ratio, zbb, sigmax(500), sigma1(500), tau(500)
real taumax(500), theta(500)
real mises(500), sigma2(500)
character*6 plot
character*1 respon
```

```

open(unit=52,file='osablat',status='unknown')
open(unit=53,file='ostress',status='unknown')
open(unit=54,file='obeam',status='unknown')

c Read Input Parameters
print*, 'SABLAT- Structural Analysis Code for the Ablative'
print*, ' in the Uptake of the VLS'
print*, ' '
print*, 'Input the Tensile Modulus of the Ablative (Msi):'
read(*,102)eat
print*, 'Input the Compressive Modulus of the Ablative:'
read(*,102)eac
print*, 'Input the thickness of the ablative (in):'
print*, '(recommended thickness= 0.38 in)'
read(*,103)ha
print*, 'Input the tensile strength of the ablative (ksi):'
read(*,104)sut
print*, 'Input the compressive strength of the ablative (ksi):'
read(*,104)suc
103 format(f20.10)
104 format(f20.10)
c Convert to psi
eat=eat*1.0e6
eac= eac*1.0e6
sut= sut*1000.
suc= suc*1000.
print*, 'Is the adhesive layer to be included in this run?(y/n)'
read(*,101)respon
101 format(a)
if(respon .eq. 'y')then
print*, 'Input the tensile modulus of the adhesive (Msi):'
read(*,102)egt
print*, 'Input the compressive modulus of the adhesive (Msi):'
read(*,102)egc
102 format(f20.10)
c Convert to psi
egc= egc*1.0e6
egt= egt*1.0e6
print*, 'Input the thickness of the adhesive (in):'
read(*,103)hg
else
hg= 0.0
egt= 30.0e6
egc= 30.0e6
endif
print*, 'Input the pressure acting on the beam (lbf/in):'
print*, '(recommended pressure= 824.25 lbf/in)'
read(*,105)qo
print*, 'Input the length of the beam (in):'
print*, '(recommended length= 27.75 in)'
read(*,105)length

```

c Input Constant Steel Section Properties & Dimensions (for

```

c subroutine mofi)
es= 30.0e6
width= 8.54
hs= 0.105
wc= 4.03
hc= 0.12
wb= 0.12
hb= 1.34

call mofi(eat,eac,egt,egc,ha,hg,es,width,hs,wc,hc,wb,
*hb,mofin,mofip,ybarn, ybarp,zbarn,zbarp,qo,length,respon)

call cbeam(es,mofin,mofip,length,qo,deflect,dwdx,moment
*,shear,posit,nsteps,a)

c CALCULATE BENDING STRESSES ON TOP SURFACE
write(53,106)
write(53,106)
write(53,109)
write(53,106)
write(53,107)
write(53,108)
106 format(' ')
109 format('BENDING STRESS ON TOP SURFACE OF ABLATIVE')
107 format(' X(in) bstress(ksi)')
108 format('-----')

c Calculate Stresses in Ablative
do 601 i=1,nsteps
if(posit(i) .le. a)then
c (top is in tension, use negative moment values)
ctop= (hs+ hg+ ha)- ybarn
cbottom= hs+ hg- ybarn
zbb= zbarn
inertia= mofin
ratio=eat/es
goto 612
endif

if(posit(i) .le. (length-a))then
c (top is in compression, use positive moment values)
ctop= (hs+ hg+ ha)- ybarp
cbottom= hs+ hg- ybarp
zbb= zbarp
inertia= mofip
ratio= eac/es
goto 612
endif

ctop= (hs+ hg+ ha)- ybarn
cbottom= hs+ hg- ybarn
zbb= zbarn
inertia= mofin
ratio= eat/es

```

```

c BENDING STRESS ON TOP SURFACE OF ABLATIVE
612 bstress(i)= moment(i)*ctop/(inertia*1000.)
bstress(i)= -bstress(i)*ratio

c BENDING STRESS ON BOTTOM SURFACE OF ABLATIVE
sigmax(i)= moment(i)*cbottom/(inertia*1000.)
sigmax(i)= -sigmax(i)*ratio

c SHEAR STRESS ON BOTTOM SURFACE OF ABLATIVE
tau(i)= shear(i)* ha*zbb*ratio/(inertia*1000.)

c EQUIVALENT UNIAXIAL STRESS ON BOTTOM OF ABLATIVE
sigma1(i)= sigmax(i)/2+ sqrt((sigmax(i)/2)**2+ tau(i)**2)
sigma2(i)= sigmax(i)/2- sqrt((sigmax(i)/2)**2+ tau(i)**2)
mises(i)= sqrt(sigma1(i)**2+sigma2(i)**2-sigma1(i)*sigma2(i))

c MAXIMUM SHEAR STRESS ON BOTTOM SURFACE
taumax(i)= sqrt(tau(i)**2+ (sigmax(i)/2)**2)

c ANGLE BETWEEN PRINCIPAL AXES AND THE X & Y AXES
theta(i)= 0.5*atan(2*tau(i)/sigmax(i))

write(53,105)posit(i),bstress(i)
601 continue
105 format(f6.3,3x,f10.6)

write(52,568)
write(52,461)bstress(1)
write(52,462)sut/1000.
write(52,463)(sut/1000.)/bstress(1)
if((sut/1000.)/bstress(1) .le. 1)then
write(52,464)
endif
write(52,468)
write(52,465)bstress((nsteps-1)/2+1)
write(52,466)-suc/1000.
write(52,467)-(-suc/1000.)/bstress((nsteps-1)/2+1)
if(abs((-suc/1000.)/bstress((nsteps-1)/2+1)) .le. 1.0)then
write(52,464)
endif

461 format('Max. Ablative Bending Stress at Ends=',f10.5,' ksi')
462 format('Ultimate Tensile Strength=',f10.5,' ksi')
463 format('Factor of Safety=',f10.5)
464 format('STRESS EXCEEDS ABLATIVE STRENGTH')
465 format('Max. Ablative Compressive Stress at Center=',f10.5,'ksi')
466 format('Ultimate Compressive Strength=',f10.5,' ksi')
467 format('Factor of Safety=',f10.5)
468 format(' ')
568 format('PEAK STRESS RESULTS:')

write(53,106)
write(53,106)
write(53,110)

```

```

write(53,106)
write(53,111)
write(53,113)
110 format(' STRESSES ON BOTTOM SURFACE OF ABLATIVE')
111 format(' X(in) SX(ksi) TX(ksi) Seq(ksi) Tmax(ksi) Theta(rad)')
113 format('-----')
do 602 i=1,nsteps
write(53,112)posit(i),sigmax(i),tau(i),mises(i),taumax(i),
*theta(i)
602 continuc
112 format(f6.3,2x,f7.4,2x,f7.4,2x,f7.4,3x,f7.4,4x,f7.4)

stop
end

c#####i,#####
subroutine mofi(eat,eac,egt,egc,ha,hg,es,width,hs,wc,hc,wb,
*hb,mofin,mofip,ybarn, ybarp,zbarn,zbarp,qo,length,respon)
c 4/30/92- Calculating moment of inertia for the cross section
c of a beam model of the uptake. Assume have 4 layers:
c an ablative, an adhesive, a steel plate, and a C
c channel. Assume have different properties in tension
c & compression for the ablative and adhesive layers.

implicit none
real qo,length
character*1 respon
c Material Properties
real eac, eat, egc, egt, es
c Geometric Properties
real w, wgc,wgt, wac, wat, wc, wb, hc, hb, hs, hg, ha
real hg1a, hg1b, hg1, hg2, wg1, wg2, width
real wa1, wa2, wg, ha1, ha1a, ha1b, ha2, wa
c Section properties
real sumarea, summy, ybarp,ybarn, sumiy, sumicg
real mofip, mofin
c Ablative centroid
real zbarn, zbarp
c Miscel. Variables
real dd, ee, ff, gg, hh, jj, uu, vv, ww
real alpha, beta, gamma, delta, epsilon, tau, lambda, psi

w= width

cNOMENCLATURE
c eac= ablative's elastic modulus in compression (psi)
c eat= ablative's elastic modulus in tension (psi)
c egc= adhesive's elastic modulus in compression (psi)
c egt= adhesive's elastic modulus in tension (psi)
c es= elastic modulus of steel (psi)
c ha= thickness of ablative layer
c ha1= thickness of ablative below the neutral axis (in)
c ha2= thickness of ablative above the neutral axis (in)
c hb= thickness of steel sidewalls (in)

```

c hc= thickness of steel endwall (in)
 c hg= thickness of glue layer (in)
 c hg1= thickness of glue below neutral axis when neutral axis
 c passes through the adhesive layer (in)
 c hg2= thickness of glue above neutral axis when neutral axis
 c passes through the adhesive layer (in)
 c hs= thickness of steel plate (in)
 c mofin= composite moment of inertia under a negative moment (in⁴)
 c mofip= composite moment of inertia under a positive moment (in⁴)
 c sumarea= sum of areas in cross section (in²)
 c sumicg= sum of moments of inertia about centers of gravity (in⁴)
 c sumiy= sum of 2nd moments of inertia (in⁴)
 c summy= sum of 1st moments, My (A*y) (in³)
 c w= assumed width of steel plate (in)
 c wa1= effective width of ablative below neutral axis (in)
 c wa2= effective width of ablative below neutral axis (in)
 c wac= effective width of ablative in compression (in)
 c wat= effective width of ablative in tension (in)
 c wb= width of steel sidewalls in c-channel (in)
 c wc= width of steel endwall in c-channel (in)
 c wgc= effective width of glue in compression (in)
 c wgt= effective width of glue in tension (in)
 c ybarn= location of neutral axis under a negative moment (in)
 c ybarp= location of neutral axis under a positive moment (in)
 c zbarn= distance of centroid of ablative from ybarn (in)
 c zbarp= distance of centroid of ablative from ybarp (in)

c Calculate Equivalent cross sectional widths

wac= w*(eac/es)
 wgc= w*(egc/es)
 wat= w*(eat/es)
 wgt= w*(egt/es)

c Echo Material & Section Properties

write(52,392)
 write(52,199)qo
 write(52,391)length
 write(52,114)
 write(52,393)
 write(52,104)es
 write(52,131)hs
 write(52,394)w
 write(52,132)hb
 write(52,395)wb
 write(52,133)hc
 write(52,396)wc
 write(52,114)
 if(respon.eq. 'y')then
 write(52,397)
 write(52,105)egt
 write(52,106)egc
 write(52,130)hg
 write(52,390)wgc
 write(52,135)wgt

```

endif
write(52,114)
write(52,398)
write(52,107)eat
write(52,108)eac
write(52,109)ha
write(52,389)wac
write(52,134)wat
write(52,114)

392 format('FIXED-FIXED BEAM LOADING AND LENGTH')
199 format('Pressure=',f15.4,' lbf/in')
391 format('Length=',f10.4,' in')
393 format('STEEL SECTION PROPERTIES')
104 format('Elastic Modulus of Steel=',f15.2,'psi')
131 format('Thickness of Steel Plate=',f6.4,' in')
394 format('Width of Steel Plate=',f6.4,' in')
132 format('C-Channel Sidewalls: Height= ',f6.4,' in')
395 format(' Width =',f6.4,' in')
133 format('C-Channel Endwall: Height= ',f6.4,' in')
396 format(' Width =',f6.4,' in')
397 format('ADHESIVE LAYER PROPERTIES')
105 format('Tensile Modulus of Adhesive=',f15.2,'psi')
106 format('Compressive Modulus of Adhesive=',f15.2,'psi')
130 format('Adhesive Thickness=',f6.4,' in')
390 format('Effective Adhesive Width (Compression)=',f6.4,' in')
135 format('Effective Adhesive Width (tension)=',f6.4,' in')
398 format('ABLATIVE LAYER PROPERTIES')
107 format('Tensile Modulus of Ablative=',f15.2,'psi')
108 format('Compressive Modulus of Ablative=',f15.2,'psi')
109 format('Ablative Thickness=',f6.4,' in')
389 format('Effective Ablative Width (Compression)=',f6.4,' in')
134 format('Effective Ablative Width (tension)=',f6.4,' in')
114 format(' ')

```

cMAKE CALCULATIONS ASSUMING A POSITIVE MOMENT

c CASE 1 Assume neutral axes goes thru steel & positive moment
c (top surface in compression)

```

sumarea= ha*wac+ hg*wg+ hs*w+ 2*hb*wb+ hc*wc
c print*,sum(A),steel=',sumarea,'in^2'

```

```

summy= ha*wac*(hs+hg+ha/2)+ hg*wg*(hs+hg/2)+ hs**2*w/2
summy= summy-hb**2*wb+ hc*wc*(hc/2- hb)

```

```

c print*,sum(My),steel=',sum,my,'in^3'

```

c Determine neutral axis location
ybarp= summy/sumarea

```

c print*,ybarp,steel=',ybarp,'in'

```

```

zbarp= (hs+ hg+ ha)- ybarp- ha/2

```

```
sumiy= ha*wac*(hs+hg+ha/2)**2+ hg*wg*(hs+hg/2)**2+ hs**3*w/4
sumiy= sumiy+ hb**3*wb/2+ hc*wc*(hc/2-hb)**2
```

```
sumicg=(wac*ha**3+ wg*hg**3+ w*hs**3+ 2*wb*hb**3+ wc*hc**3)/12
```

```
mofip= sumiy+ sumicg- ybarp**2*sumarea
if(ybarp .gt. hs)goto 200
```

```
goto 900
```

```
c CASE 3 Assume neutral axis goes thru adhesive & positive moment
c (top surface in compression)
```

```
200 wgl= wgt
```

```
wg2= wgc
```

```
wa= wac
```

```
c If wgl= wg2 (egt=egc), then use same cross section as case 1
```

```
c Section properties (i.e. ybar) will also be the same
```

```
if(wgl .lt. (wg2+ wg2/100000.))then
```

```
if(wgl .gt. (wg2- wg2/100000.))then
```

```
c Check if ybar is above the glue layer
```

```
if(ybarp .gt. (hs+hg))goto 300
```

```
goto 900
```

```
endif
```

```
endif
```

```
c Set constants
```

```
dd= ha*wa+ hs*w+ 2*hb*wb+ hc*wc
```

```
ee= ha*wa*(hs+hg+ha/2)+ hs**2*w/2-hb**2*wb+hc*wc*(hc/2-hb)
```

```
ff= ee+ wg2*hg*hs+ wg2*hg**2/2
```

```
gg= (wgl- wg2)*hs
```

```
hh= (wgl- wg2)/2
```

```
jj= ha*wa*(hs+ hg+ ha/2)**2+ hs**3*w/4+ hb**3*wb/2
```

```
jj= jj+hc*wc*(hc/2- hb)**2
```

```
uu= wgl- wg2- hh
```

```
vv= hs*wgl- hs*wg2+ dd+ hg*wg2- gg
```

```
ww= dd*hs+ wg2*hg*hs- ff
```

```
c Calculate hgl & hg2
```

```
hgl1a= (-vv+ sqrt(vv**2- 4*uu*vv))/(2*uu)
```

```
hgl1b= (-vv- sqrt(vv**2- 4*uu*vv))/(2*uu)
```

```
if(hgl1a .ge. hgl1b)then
```

```
hgl= hgl1a
```

```
else
```

```
hgl= hgl1b
```

```
endif
```

```
hg2= hg- hgl
```

```
if(hg2 .lt. 0.0)then
```

```
if(hgl1a .ge. hgl1b)then
```

```
hgl= hgl1b
```

```
hg2= hg- hgl
```

```
else
```

```
hgl= hgl1a
```

```
hg2= hg- hgl
```

```
endif
endif
```

```
c Now, if either hg1 or hg2 is lt 0, must go to next layer
if(hg1 .lt. 0.0)goto 300
if(hg2 .lt. 0.0)goto 300
```

```
c Calculate neutral axis location and check it
ybarp= hs+ hg1
zbarp= (hs+hg+ha)- ybarp- ha/2
```

```
c Calculate other section properties
sumarea= dd+ wg2*hg+ (wg1-wg2)*hg1
sumiy= jj+ (hg-hg1)*wg2*(hs+ hg1+ hg/2- hg1/2)**2
sumiy= sumiy+ hg1*wg1*(hs+hg1/2)**2
```

```
sumicg= (wa*ha**3+ wg2*hg2**3+ wg1*hg1**3+ w*hs**3)
sumicg= (sumicg+ 2*wb*hb**3+ wc*hc**3)/12
```

```
mofip= sumiy+ sumicg- ybarp**2*sumarea
```

```
c Check location of neutral axis
if(ybarp .gt. (hs+hg))goto 300
goto 900
```

```
c CASE 5 Assume neutral axis goes thru ablative & positive moment
```

```
c (top surface in compression)
```

```
300 wa2= wac
```

```
wa1= wat
```

```
wg= wgt
```

```
c If wa1=wa2 (eat=eac) then have same section properties as
```

```
c previous case
```

```
if(wa1 .lt. (wa2+ wa2/100000.))then
```

```
if(wa1 .gt. (wa2- wa2/100000.))then
```

```
c Check location of neutral axis
```

```
if(ybarp .gt. (ha+hg+hs))goto 787
```

```
goto 900
```

```
endif
```

```
endif
```

```
c Set Constants
```

```
alpha= ha*wa2+ hg*wg+ hs*w+ 2*hb*wb+ hc*wc
```

```
beta= wa1- wa2
```

```
gamma= ha*hs*wa2+ ha*wa2*hg+ (ha**2)*wa2/2+ hg*wg*hs+
* (hg**2)*wg/2+ (hs**2)*w/2- wb*(hb**2)+ (hc**2)*wc/2- hb*hc*wc
```

```
delta= (hs+hg)*wa1- (hs+ hg)*wa2
```

```
epsilon= (wa1- wa2)/2
```

```
tau= epsilon- beta
```

```
lambda= delta- alpha- beta*hs- beta*hg
```

```
psi= gamma- alpha*hs- alpha*hg
```

```
c Calculate ha1 & ha2
```

```
ha1a= (-lambda+sqrt(lambda**2-4*tau*psi))/(2*tau)
```

```
ha1b= (-lambda-sqrt(lambda**2-4*tau*psi))/(2*tau)
```

```

if(ha1a .gt. ha1b)then
  ha1= ha1a
else
  ha1= ha1b
endif

```

```

ha2= ha- ha1
if(ha2 .lt. 0.0)then
  if(ha1a .gt. ha1b)then
    ha1= ha1b
    ha2= ha-ha1
  else
    ha1= ha1a
    ha2= ha- ha2
  endif
endif

```

c Calculate Neutral Axis Location & Check It

```

ybarp= hs+ hg +ha1
zbarp= (hs+ hg+ ha)- ybarp- ha/2

```

```

if(ybarp .gt. (hs+hg+ha))then
  787 print*, '!!!!!!!!!!!!!! ERROR !!!!!!!!!!!!!!!'
  print*, 'ybarp is above top of section'
  print*, ' ybarp=', ybarp, 'in'
  write(52,125)
  write(52,126)
  write(52,127)ybarp
  125 format('!!!!!!!!!!!!!! ERROR !!!!!!!!!!!!!!!')
  126 format('ybarp is above top of section')
  127 format(' ybarp=', f20.10, 'in')
  goto 999
endif

```

c Calculate Other Section Properties

```

sumarea= alpha+ beta*ha1
sumiy= ha2*wa2*(hs+ hg+ ha1+ ha2/2)**2+ ha1*wa1*(hs+hg+ha1/2)**2
sumiy= sumiy+ hg*wg*(hs+hg/2)**2+ w*hs**3/4+ wb*hb**3/2
sumiy= sumiy+ hc*wc*(hc/2- hb)**2
sumicg= (wa2*ha2**3+ wa1*ha1**3+ wg*hg**3+ w*hs**3)
sumicg= (sumicg+ 2*wb*hb**3+ wc*hc**3)/12
mofip= sumiy+ sumicg- (ybarp**2)*sumarea

```

c#####
cMAKE CALCULATIONS ASSUMING A NEGATIVE MOMENT

c CASE 2 Assume neutral axes goes thru steel & negative moment

c (top surface in tension)

```

900 sumarea= ha*wa1+ hg*wg1+ hs*w+ 2*hb*wb+ hc*wc

```

```

summy= ha*wa1*(hs+hg+ha/2)+ hg*wg1*(hs+hg/2)+ hs**2*w/2
summy= summy-hb**2*wb+ hc*wc*(hc/2- hb)

```

c Determine neutral axis location
 $y_{barn} = \text{summy} / \text{sumarea}$

$z_{barn} = (hs + hg + ha) - y_{barn} - ha/2$

$\text{sumiy} = ha * wa * (hs + hg + ha/2)^2 + hg * wgt * (hs + hg/2)^2 + hs^3 * w/4$
 $\text{sumiy} = \text{sumiy} + hb^3 * wb/2 + hc * wc * (hc/2 - hb)^2$

$\text{sumicg} = (wa * ha^3 + wgt * hg^3 + w * hs^3 + 2 * wb * hb^3 + wc * hc^3) / 12$

$\text{mofin} = \text{sumiy} + \text{sumicg} - y_{barn}^2 * \text{sumarea}$

c Check to see if neutral axis passes thru steel
 if($y_{barn} .gt. hs$) goto 600

goto 999

c CASE 4 Assume neutral axis goes thru adhesive & negative moment

c (top surface in tension)

600 $wg1 = wgc$

$wg2 = wgt$

$wa = wat$

c If $wg1 = wg2$ (egc=egt) then use same sxn properties as before

if($wg1 .lt. (wg2 + wg2/100000.)$) then

if($wg1 .gt. (wg2 - wg2/100000.)$) then

if($y_{barn} .gt. (hs + hg)$) goto 800

goto 999

endif

endif

c Set constants

$dd = ha * wa + hs * w + 2 * hb * wb + hc * wc$

$ee = ha * wa * (hs + hg + ha/2) + hs^2 * w/2 - hb^2 * wb + hc * wc * (hc/2 - hb)$

$ff = ee + wg2 * hg * hs + wg2 * hg^2/2$

$gg = (wg1 - wg2) * hs$

$hh = (wg1 - wg2)/2$

$jj = ha * wa * (hs + hg + ha/2)^2 + hs^3 * w/4 + hb^3 * wb/2$

$jj = jj + hc * wc * (hc/2 - hb)^2$

$uu = wg1 - wg2 - hh$

$vv = hs * wg1 - hs * wg2 + dd + hg * wg2 - gg$

$ww = dd * hs + wg2 * hg * hs - ff$

c Calculate $hg1$ & $hg2$

$hg1a = (-vv + \sqrt{vv^2 - 4 * uu * vv}) / (2 * uu)$

$hg1b = (-vv - \sqrt{vv^2 - 4 * uu * vv}) / (2 * uu)$

if($hg1a .ge. hg1b$) then

$hg1 = hg1a$

else

$hg1 = hg1b$

endif

$hg2 = hg - hg1$

if($hg2 .lt. 0.0$) then

```

if(hg1a .ge. hg1b)then
  hg1= hg1b
  hg2= hg- hg1
else
  hg1= hg1a
  hg2= hg- hg1
endif
endif
c Now, if either hg1 or hg2 is lt 0, must go to next layer
if(hg1 .lt. 0.0)goto 800
if(hg2 .lt. 0.0)goto 800

c Calculate neutral axis location and check it
ybarn= hs+ hg1
zbarn= (hs+ hg+ ha)- ybarn- ha/2

c Calculate other section properties
sumarea= dd+ wg2*hg+ (wg1-wg2)*hg1
sumiy= jj+ (hg-hg1)*wg2*(hs+ hg1+ hg/2- hg1/2)**2
sumiy= sumiy+ hg1*wg1*(hs+hg1/2)**2

sumicg= (wa*ha**3+ wg2*hg2**3+ wg1*hg1**3+ w*hs**3)
sumicg= (sumicg+ 2*wb*hb**3+ wc*hc**3)/12

mofin= sumiy+ sumicg- ybarn**2*sumarea
c Check location of neutral axis
if(ybarn .gt. (hs+hg))goto 800

goto 999

c CASE 6 Assume neutral axis goes thru ablative & negative moment
c (top surface in tension)
800 wa2= wat
wa1= wac
wg= wgc
c If wa1=wa2, then eat=eac and have same sxn properties
if(wa1 .lt. (wa2+wa2/100000.))then
  if(wa1 .gt. (wa2-wa2/100000.))then
    if(ybarn .gt. (hs+hg+ha))goto 797
  goto 999
endif
endif

c Set Constants
alpha= ha*wa2+ hg*wg+ hs*w+ 2*hb*wb+ hc*wc
beta= wa1- wa2
gamma= ha*hs*wa2+ ha*wa2*hg+ (ha**2)*wa2/2+ hg*wg*hs+
* (hg**2)*wg/2+ (hs**2)*w/2- wb*(hb**2)+ (hc**2)*wc/2- hb*hc*wc
delta= (hs+hg)*wa1- (hs+ hg)*wa2
epsilon= (wa1- wa2)/2
tau= epsilon- beta
lambda= delta- alpha- beta*hs- beta*hg
psi= gamma- alpha*hs- alpha*hg

```

```

c Calculate ha1 & ha2
ha1a= (-lambda+sqrt(lambda**2-4*tau*psi))/(2*tau)
ha1b= (-lambda-sqrt(lambda**2-4*tau*psi))/(2*tau)

if(ha1a .gt. ha1b)then
ha1= ha1a
else
ha1= ha1b
endif

ha2= ha- ha1
if(ha2 .lt. 0.0)then
if(ha1a .gt. ha1b)then
ha1= ha1b
ha2= ha-ha1
else
ha1= ha1a
ha2= ha- ha2
endif
endif

c Calculate Neutral Axis Location & Check It
ybarn= hs+ hg +ha1
zbarn= (hs+ hg+ ha)- ybarn- ha/2

if(ybarn .gt. (hs+hg+ha))then
797 print*,'!!!!!! ERROR !!!!!!!!!'
print*,'ybarn is above top of section'
print*,' ybarn=',ybarn,'in'
write(52,525)
write(52,526)
write(52,527)ybarn
525 format('!!!!!!!!!!!!!! ERROR !!!!!!!!!!!!!!!')
526 format('ybarn is above top of section')
527 format(' ybarn=',f20.10,'in')
goto 999
endif

c Calculate Other Section Properties
sumarea= alpha+ beta*ha1
sumiy= ha2*wa2*(hs+ hg+ ha1+ ha2/2)**2+ ha1*wa1*(hs+hg+ha1/2)**2
sumiy= sumiy+ hg*wg*(hs+hg/2)**2+ w*hs**3/4+ wb*hb**3/2
sumiy= sumiy+ hc*wc*(hc/2- hb)**2
sumicg= (wa2*ha2**3+ wa1*ha1**3+ wg*hg**3+ w*hs**3)
sumicg= (sumicg+ 2*wb*hb**3+ wc*hc**3)/12
mofin= sumiy+ sumicg- (ybarn**2)*sumarea

999 return
end

c#####
subroutine cbeam(es,mofin,mofip,length,qo,deflect,dwdx,moment
*,shear,posit,nsteps,a)
c 5/8/92- This program solves for deflections, slopes, moments, and

```

```

c shear in a composite fixed-fixed beam loaded by a uniform
c pressure. The moment of inertia is assumed to shift from
c a value I1 to I2 when the bending moment shifts from negative
c to positive (corresponding to the moments of inertia when
c the top surface is in compression & tension).

implicit none
c Beam Properties
real length, i1, i2
c Material Properties & Load
real es, qo
c Variables Used to Find Root
real ll, nn, pp, qq, abc
real zmom(1005), fxn(1005)
real root1, root2, root3
integer i, nroot
c Coefficients Used in Deflection Eqs.
real aa, bb, cc, dd, ff, gg, hh, jj, kk, a
c Deflections/slopes/moments/shear
real x, d2wdx2, d3wdx3
real deflect(500), dwdx(500), moment(500), shear(1000)
real posit(500)
integer nsteps, n
c Inertias from mofi
real mofin, mofip

c NOMENCLATURE
c dwdx= slope of beam
c d2wdx2= 2nd derivative of deflection wrt x
c d3wdx3= 3rd derivative of deflection wrt x
c es= elastic modulus of steel (= 30e6 psi)
c i1= moment of inertia when the top surface is in tension (in^4)
c i2= moment of inertia when the top surface is in compression (in^4)
c length= length of beam (in)
c moment= bending moment in beam (in*lb)
c posit= axial position corresponding to deflection, slope, moment
c & shear matrices (in)
c qo= uniform applied pressure over the beam (lb/in)
c shear= shear in beam (lb)
c w= deflection of the beam (in)
c x= axial position along the length of the beam (in)

i1= mofin
i2= mofip

c Locate the position where moments go to zero
ll= (8- 8*(i2/i1))
nn= 6*length*(i2/i1)- 12*length
pp= 6*length**2
qq= -length**3

abc= -length/1000
nroot= 1
do 200 i=1,1001

```

```

abc= abc+ length/1000
zmom(i)= abc
fxn(i)= ll*abc**3+ nn*abc**2+ pp*abc+ qq

if(i .ge. 2)then
if(abs(fxn(i-1)+fxn(i)) .lt. abs(fxn(i-1)-fxn(i)))then
if(nroot .eq. 1)then
root1= -fxn(i-1)*(zmom(i-1)-zmom(i))/(fxn(i-1)- fxn(i))
root1= root1+ zmom(i-1)
endif

if(nroot .eq. 2)then
root2= -fxn(i-1)*(zmom(i-1)-zmom(i))/(fxn(i-1)- fxn(i))
root2= root2+ zmom(i-1)
endif

if(nroot .eq. 3)then
root3= -fxn(i-1)*(zmom(i-1)-zmom(i))/(fxn(i-1)- fxn(i))
root3= root3+ zmom(i-1)
endif
nroot= nroot+ 1
endif
endif

200 continue

c Set Root Equal to the Smallest Root
a= root1

c Calculate Values of Coefficients Needed in Solution
kk= qo/(24*es)

ff= -2*kk*length/i2
aa= -2*kk*length/i1
cc= 0.0
dd= 0.0
gg= -6*kk*length*a**2/i1+ 4*kk*a**3/i1+ 6*kk*length*a**2/i2
gg= gg- kk*length**3/i2- 4*kk*a**3/i2
gg= gg/(2*a- 2*a*(i2/i1)- length)
bb= (i2/i1)*gg
hh= kk*length**3/i2- gg*length
jj= 2*kk*length*a**3*(1/i2- 1/i1)+ a**2*(i2/i1-1)*gg
jj= jj- a*(kk*length**3/i2- gg*length)+ (kk/i1- kk/i2)*a**4

c Calculate Deflections, Slopes, Moments, and Shears
write(54,333)
write(54,334)
write(54,333)
write(54,203)
write(54,204)
333 format(' ')
334 format(' BEAM FLEXURE')
203 format('Posit.(in) Defl.(in) Slope Moment(lbf*in) Shear(lbf)')
204 format('-----')

```

```

x= -length/100
nsteps= 0
n= 0
do 201 i=1,101
x= x+ length/100
n= n+1
nsteps= nsteps+1
posit(i)= x

if(x .le. a)then
deflect(i)= aa*x**3+ bb*x**2+ cc*x+ dd+ kk*x**4/i1
dwdx(i)= 3*aa*x**2+ 2*bb*x+ cc+ 4*kk*x**3/i1
d2wdx2= 6*aa*x+ 2*bb+ 12*kk*x**2/i1
moment(i)= -es*i1*d2wdx2
d3wdx3= 6*aa+ 24*kk*x/i1
shear(i)= -es*i1*d3wdx3
goto 794
endif

if(x .le. (length/2+ 0.00001))then
deflect(i)= ff*x**3+ gg*x**2+ hh*x+ jj+ kk*x**4/i2
dwdx(i)= 3*ff*x**2+ 2*gg*x+ hh+ 4*kk*x**3/i2
d2wdx2= 6*ff*x+ 2*gg+ 12*kk*x**2/i2
moment(i)= -es*i2*d2wdx2
d3wdx3= 6*ff+ 24*kk*x/i2
shear(i)= -es*i2*d3wdx3
goto 794
endif

if(x .gt. length/2)then
n= n-2
deflect(i)= deflect(n)
dwdx(i)= -dwdx(n)
moment(i)= moment(n)
shear(i)= -shear(n)
endif

794 write(54,202)posit(i),deflect(i),dwdx(i),moment(i),shear(i)
202 format(f6.3,4x,f9.6,2x,f9.6,2x,f10.3,3x,f10.3)

201 continue

return
end

```

APPENDIX B

DEFLECTIONS AND BENDING STRESSES ON

TOP SURFACE OF BEAM VS. AXIAL POSITION

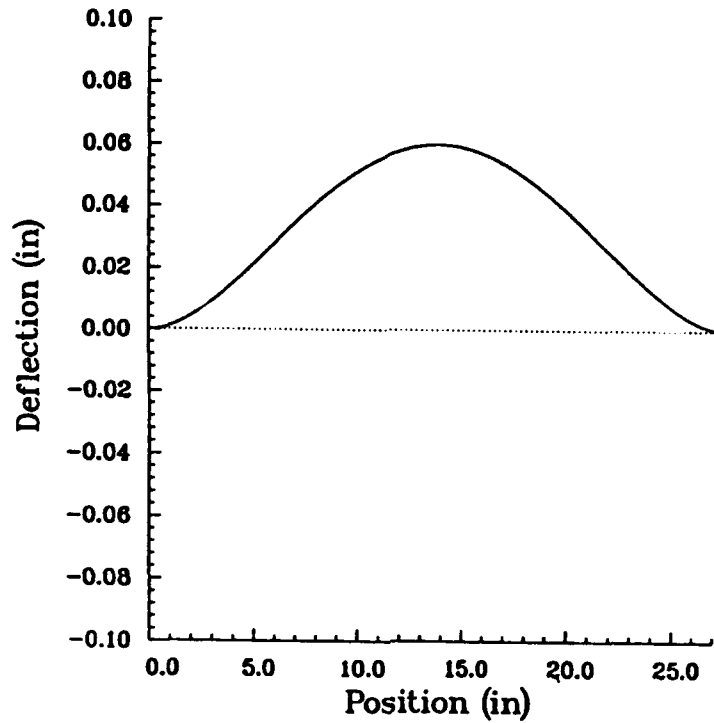


FIGURE B-1. MXBE-350 DEFLECTIONS VS. AXIAL POSITION ALONG BEAM

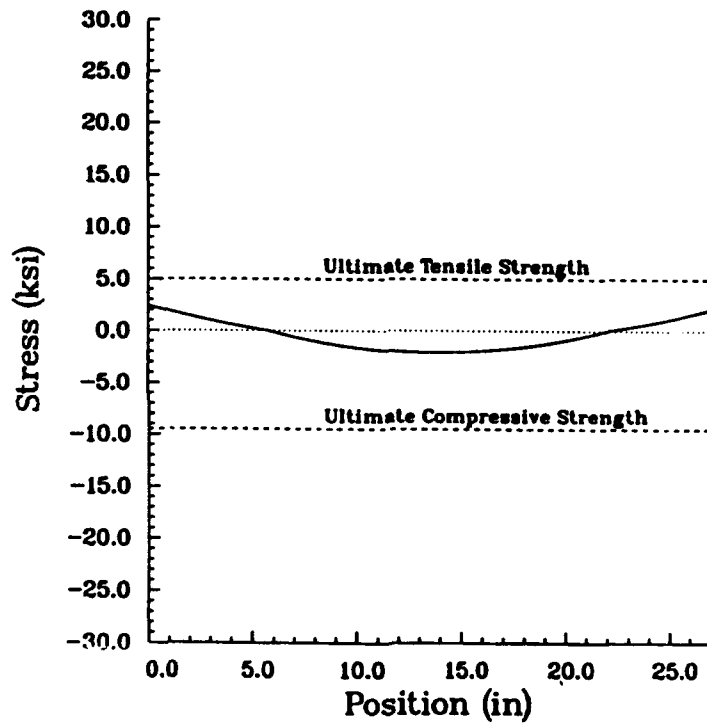


FIGURE B-2. MXBE-350 BENDING STRESSES VS. AXIAL POSITION ALONG BEAM

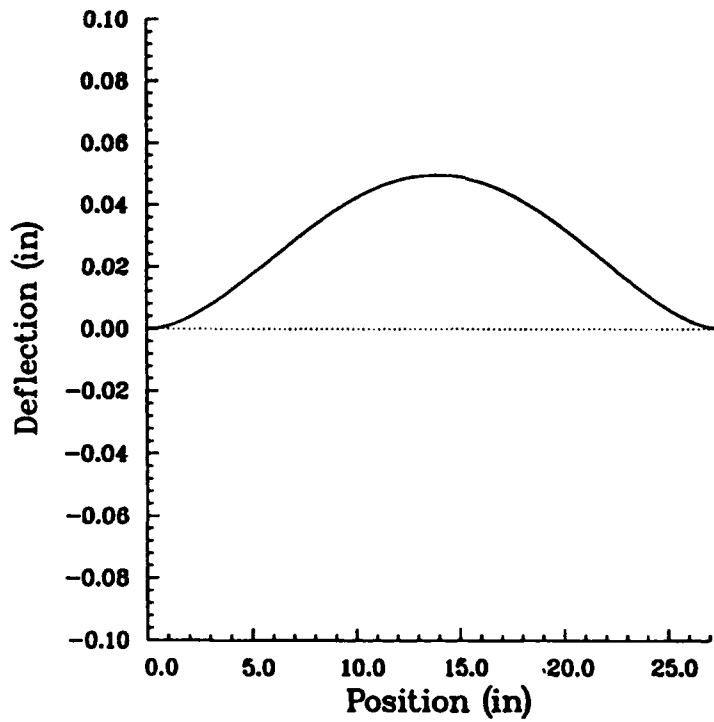


FIGURE B-3. MXB-360 DEFLECTIONS VS. AXIAL POSITION ALONG BEAM

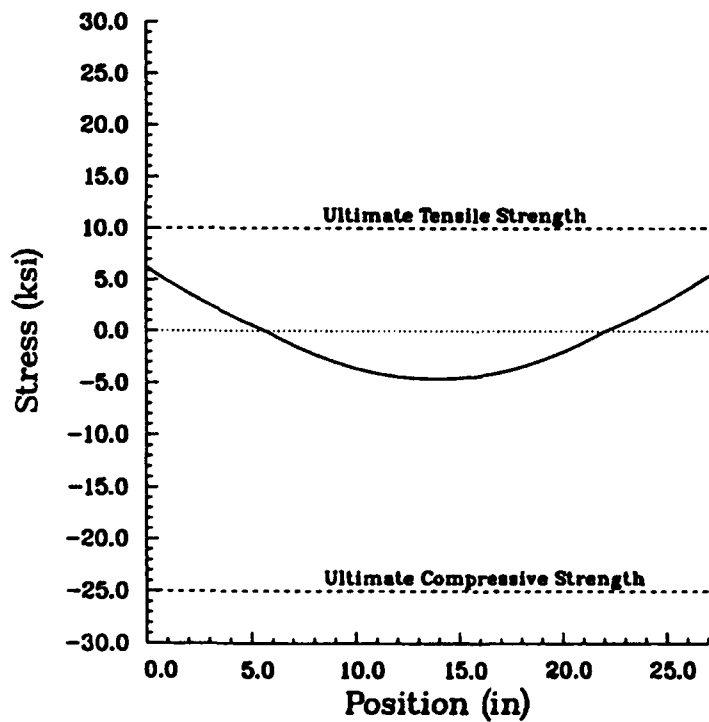


FIGURE B-4. MXB-360 BENDING STRESSES VS. AXIAL POSITION ALONG BEAM

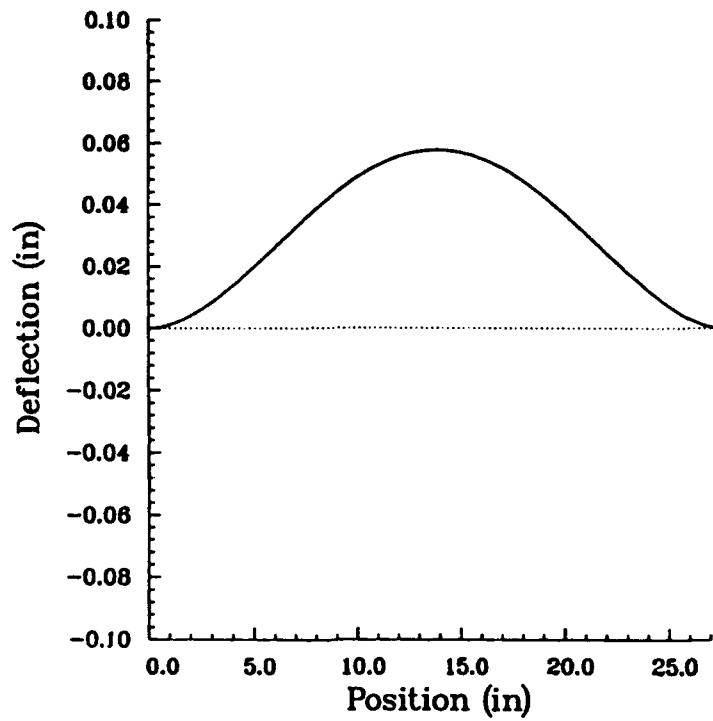


FIGURE B-5. FR-1 DEFLECTIONS VS. AXIAL POSITION ALONG BEAM

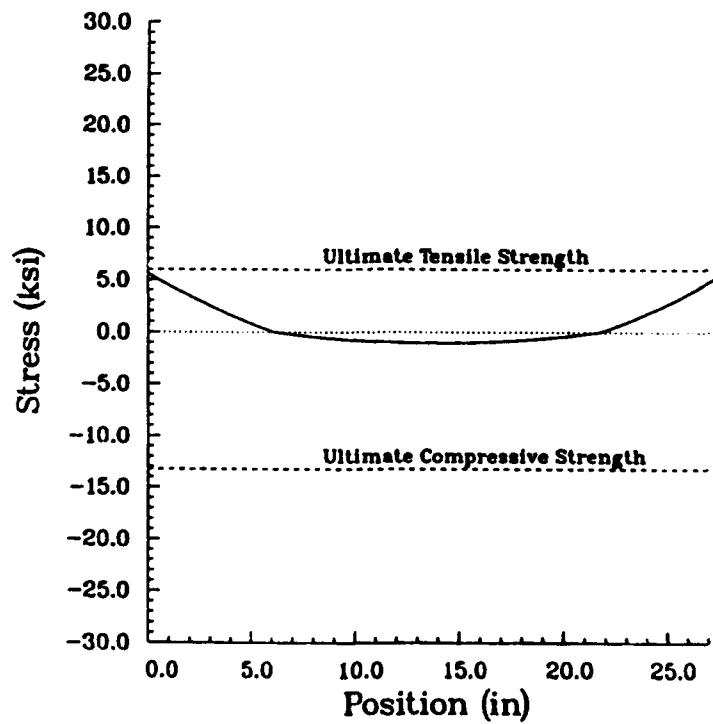


FIGURE B-6. FR-1 BENDING STRESSES VS. AXIAL POSITION ALONG BEAM

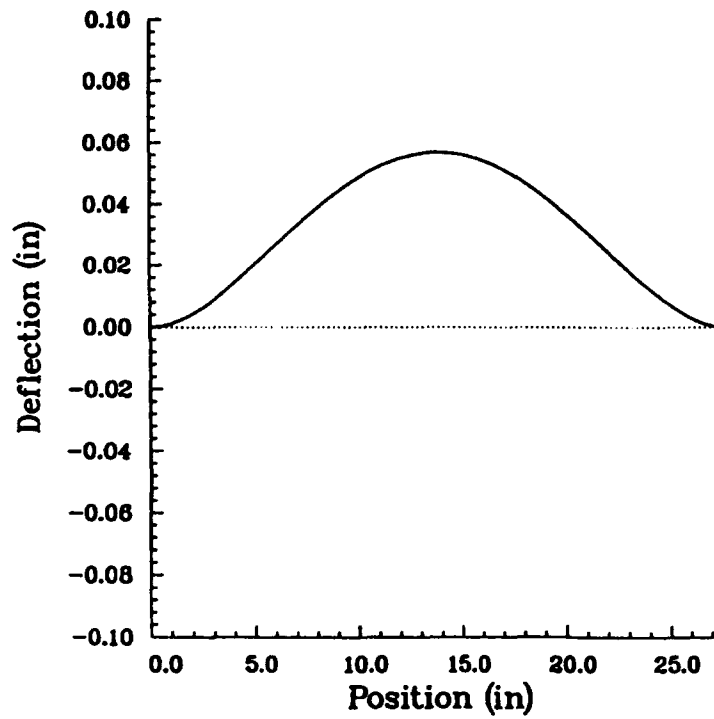


FIGURE B-7. CD208-40 DEFLECTIONS VS. AXIAL POSITION ALONG BEAM

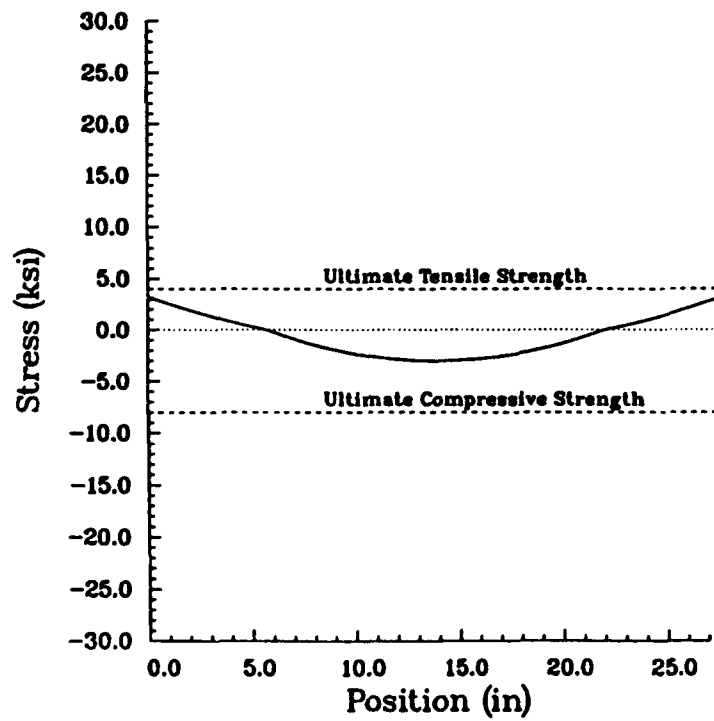


FIGURE B-8. CD208-40 BENDING STRESSES VS. AXIAL POSITION ALONG BEAM

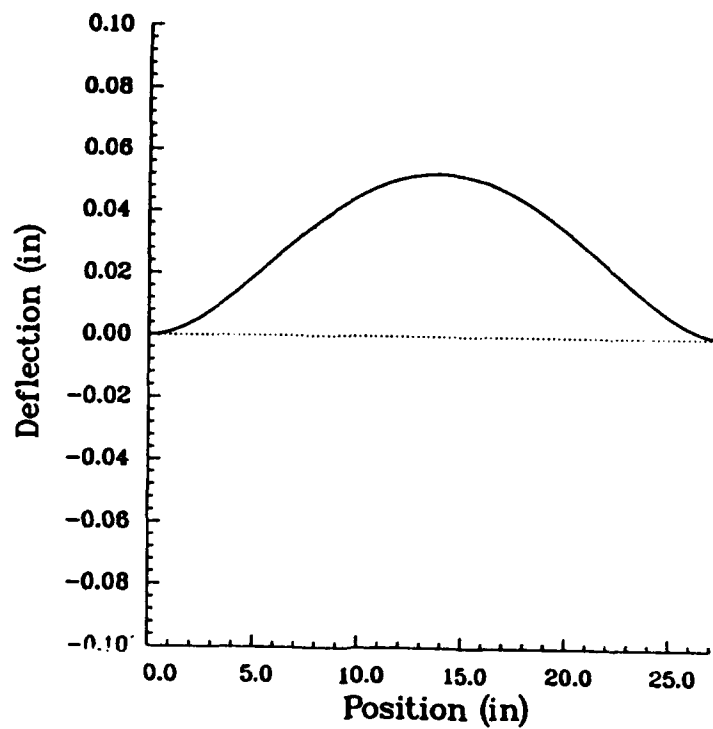


FIGURE B-9. FM16771-F DEFLECTIONS VS. AXIAL POSITION ALONG BEAM

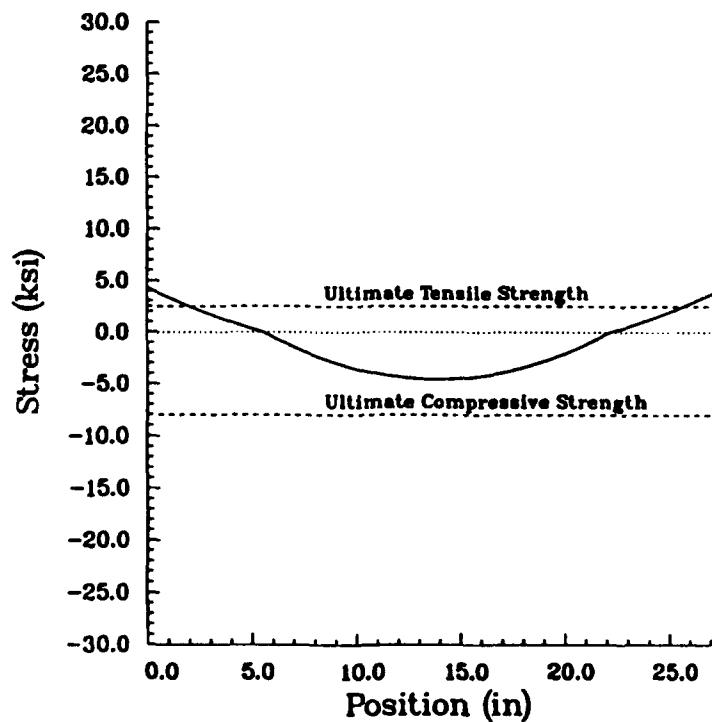


FIGURE B-10. FM16771-F BENDING STRESSES VS. AXIAL POSITION ALONG BEAM

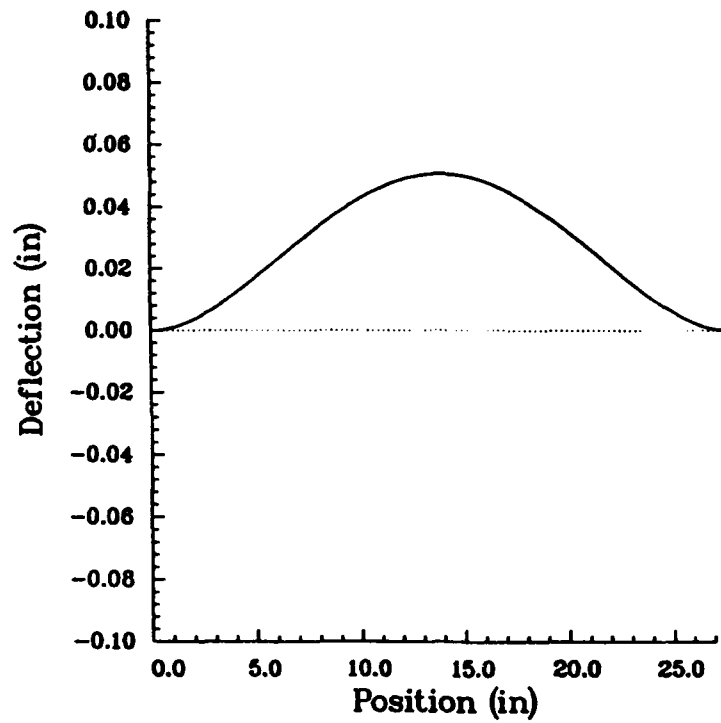


FIGURE B-11. FM16771-A DEFLECTIONS VS. AXIAL POSITION ALONG BEAM

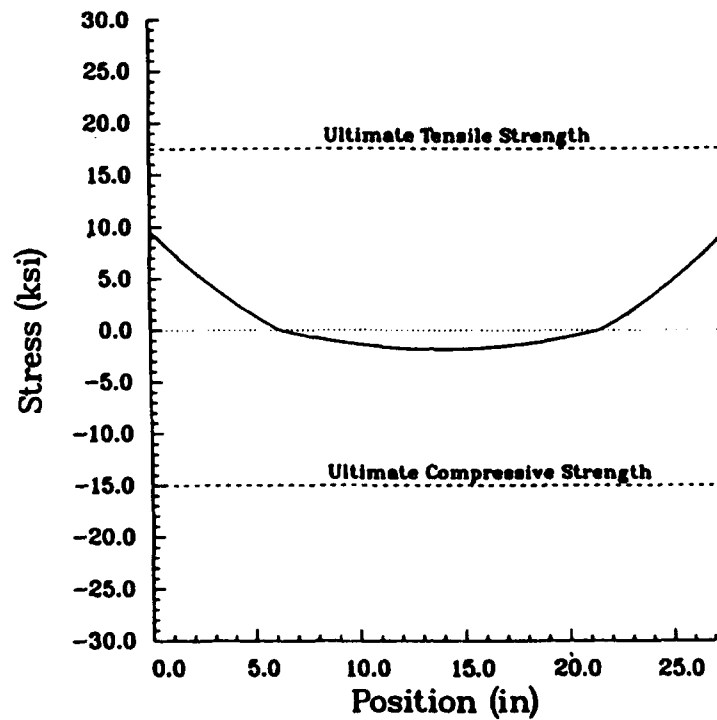


FIGURE B-12. FM16771-A BENDING STRESSES VS. AXIAL POSITION ALONG BEAM

APPENDIX C
BENDING STRESSES OF TOP SURFACE OF
BEAM VS. ABLATIVE THICKNESS

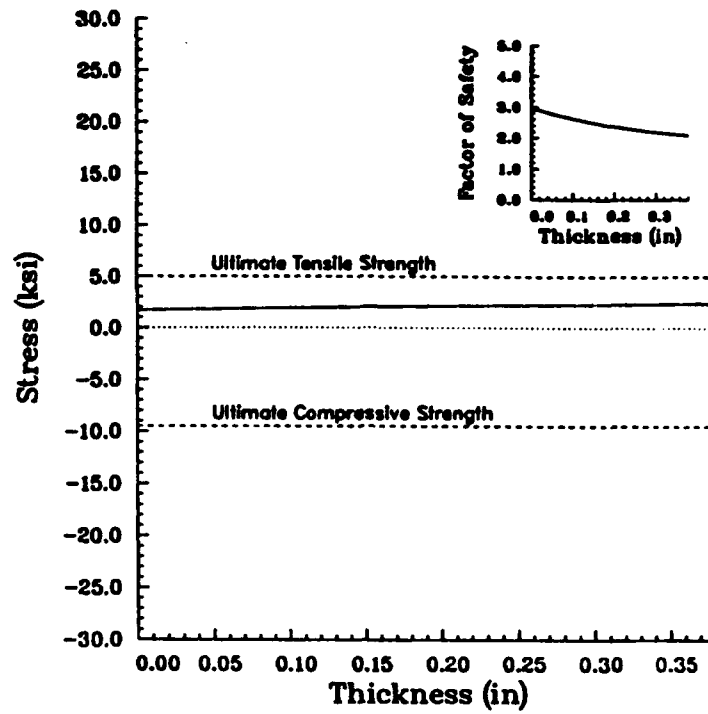


FIGURE C-1. MXBE-350 BENDING STRESSES (X=0 IN.) VS. ABLATIVE THICKNESS

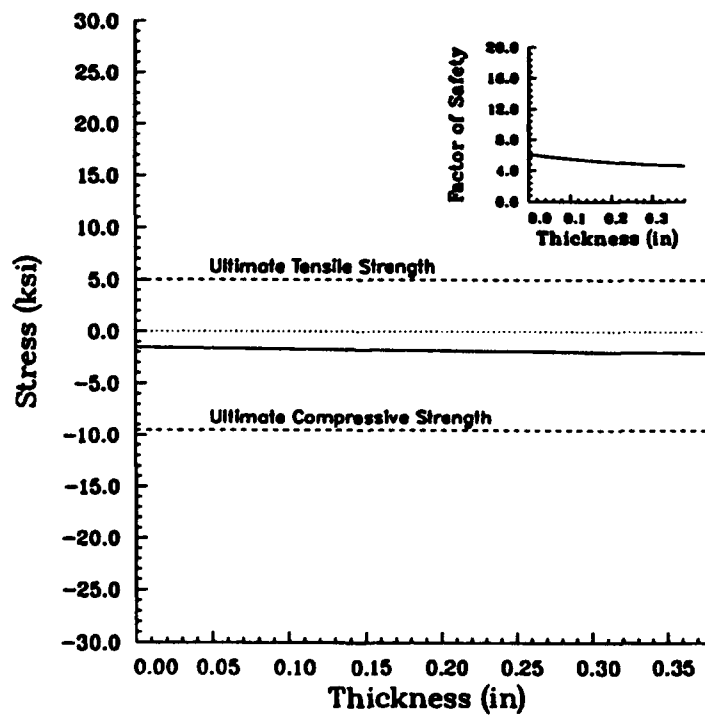
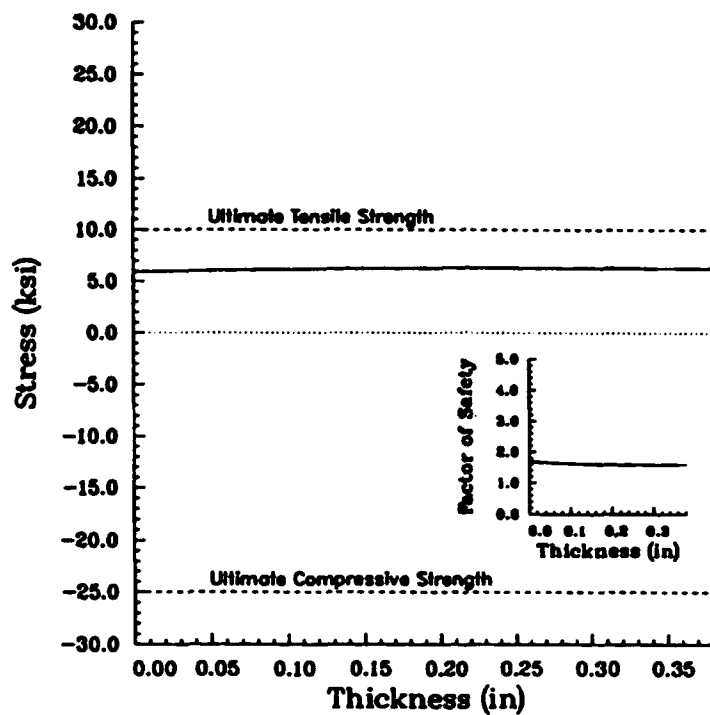
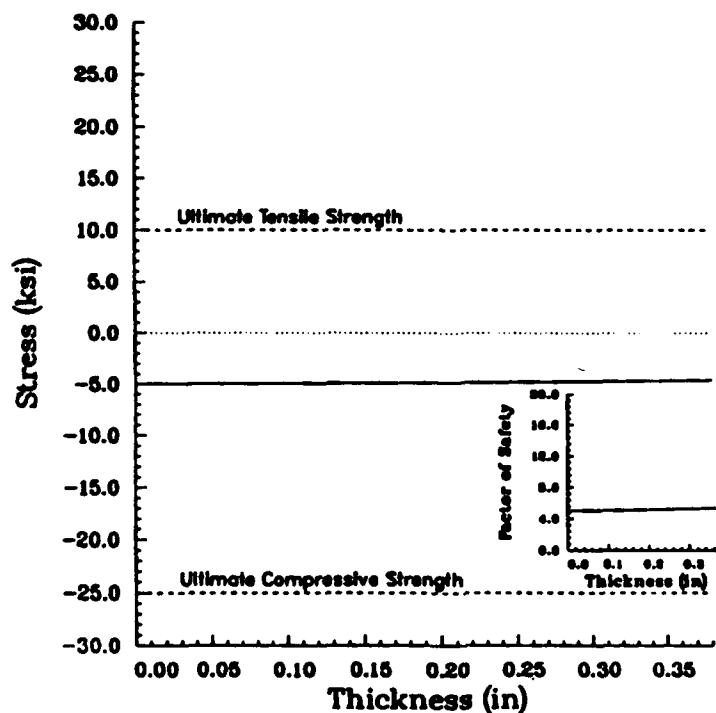


FIGURE C-2. MXBE-350 BENDING STRESSES (X=13.875 IN.) VS. ABLATIVE THICKNESS

FIGURE C-3. MXB-360 BENDING STRESSES ($X=0$ IN.) VS. ABLATIVE THICKNESSFIGURE C-4. MXB-360 BENDING STRESSES ($X=13.875$ IN.) VS. ABLATIVE THICKNESS

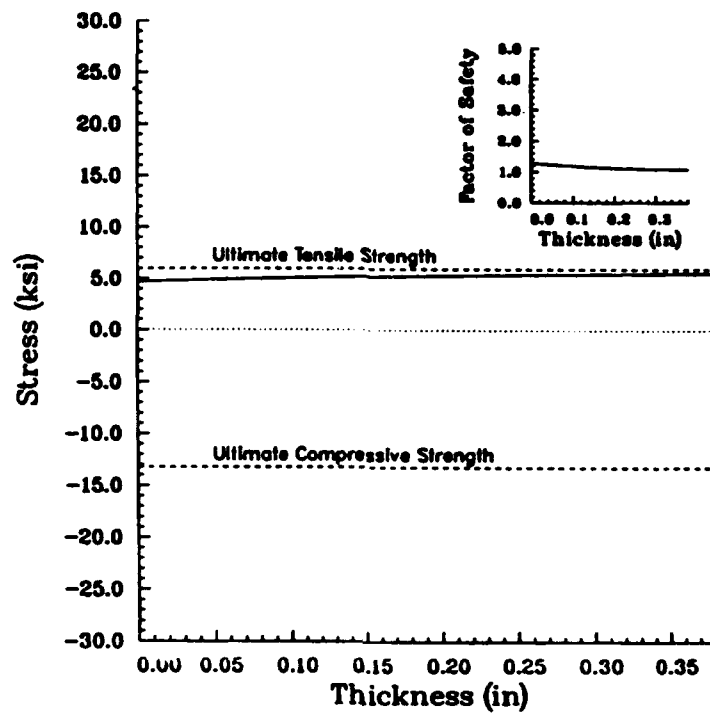


FIGURE C-5. FR-1 BENDING STRESSES ($X=0$ IN.) VS. ABLATIVE THICKNESS

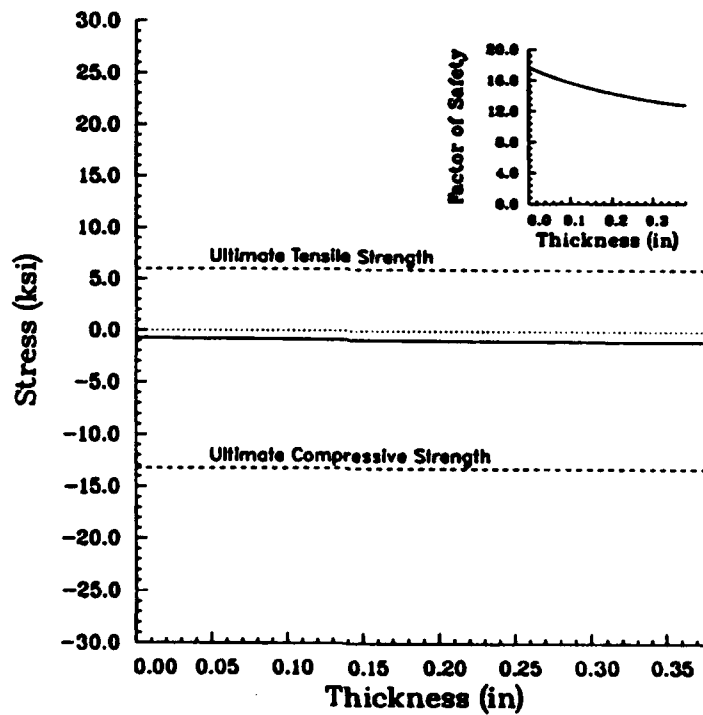


FIGURE C-6. FR-1 BENDING STRESSES ($X=13.875$) VS. ABLATIVE THICKNESS

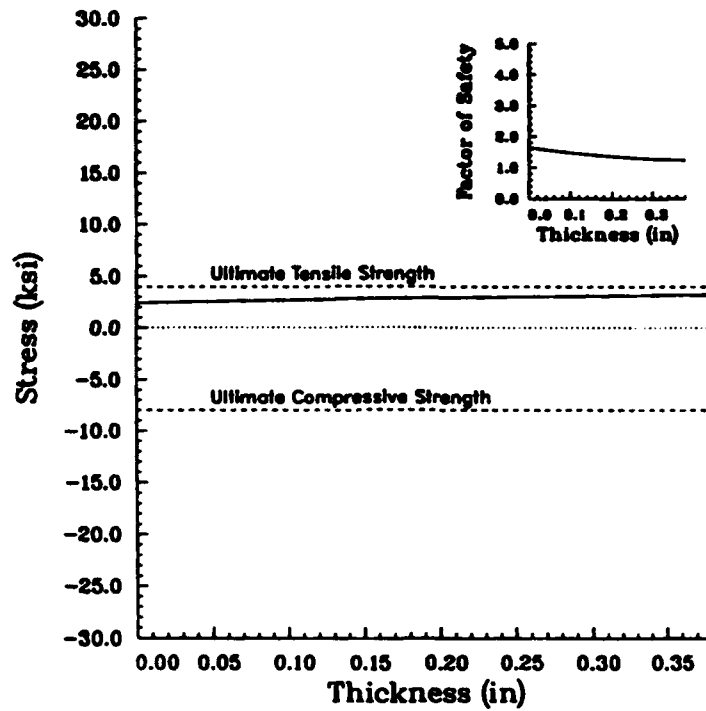


FIGURE C-7. CD208-40 (X=0 IN.) VS. ABLATIVE THICKNESS

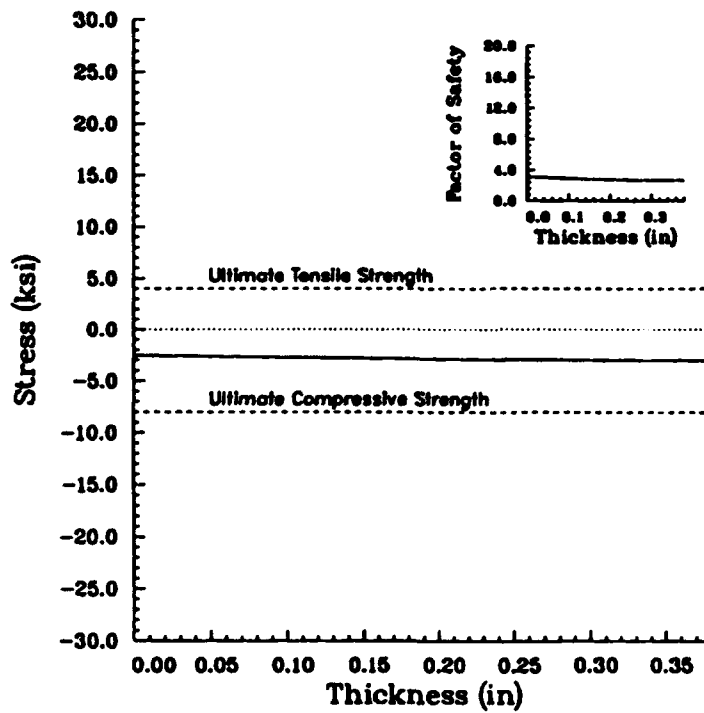


FIGURE C-8. CD208-40 BENDING STRESSES (X=13.875) VS. ABLATIVE THICKNESS

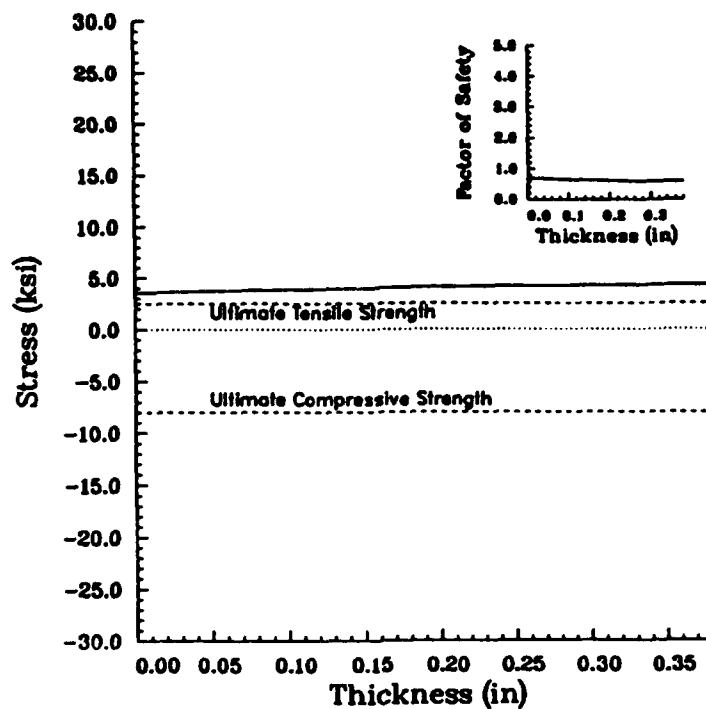


FIGURE C-9. FM16771-F BENDING STRESSES (X=0 IN.) VS. ABLATIVE THICKNESS

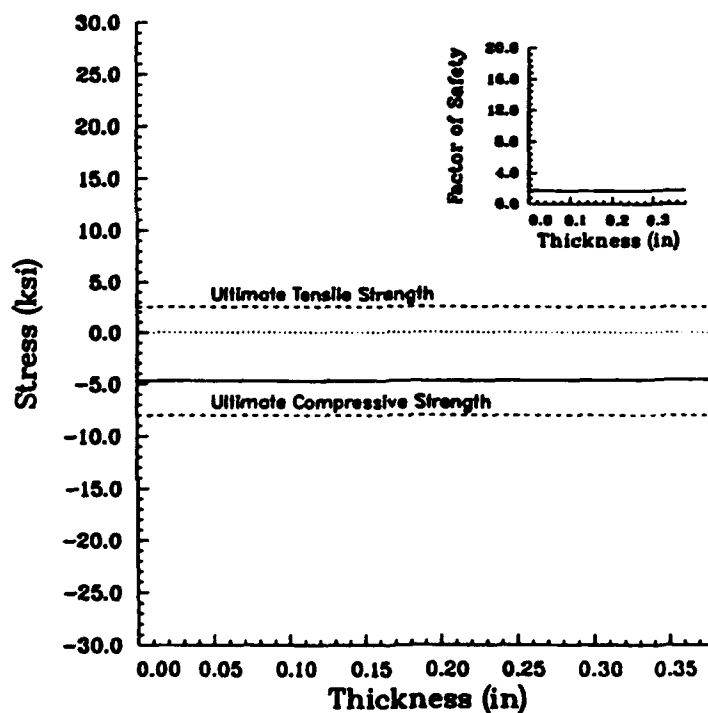
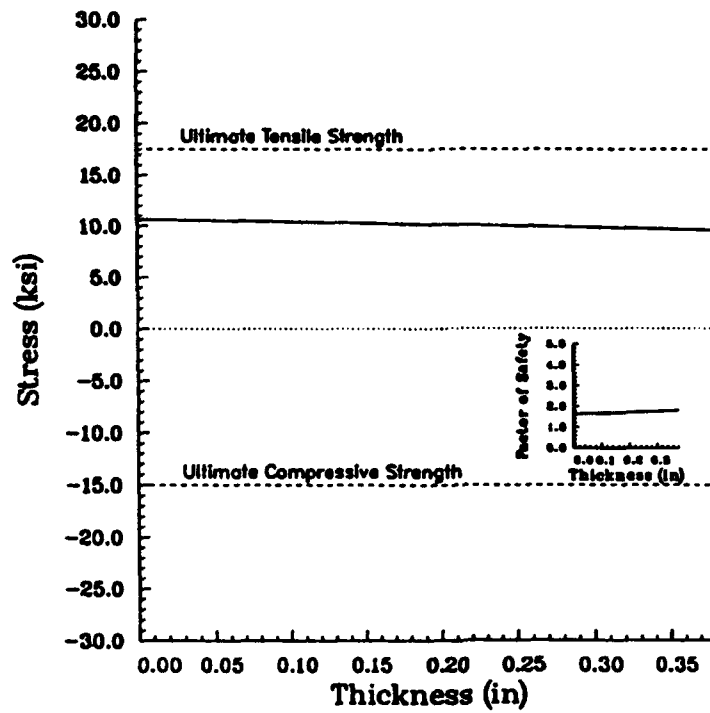
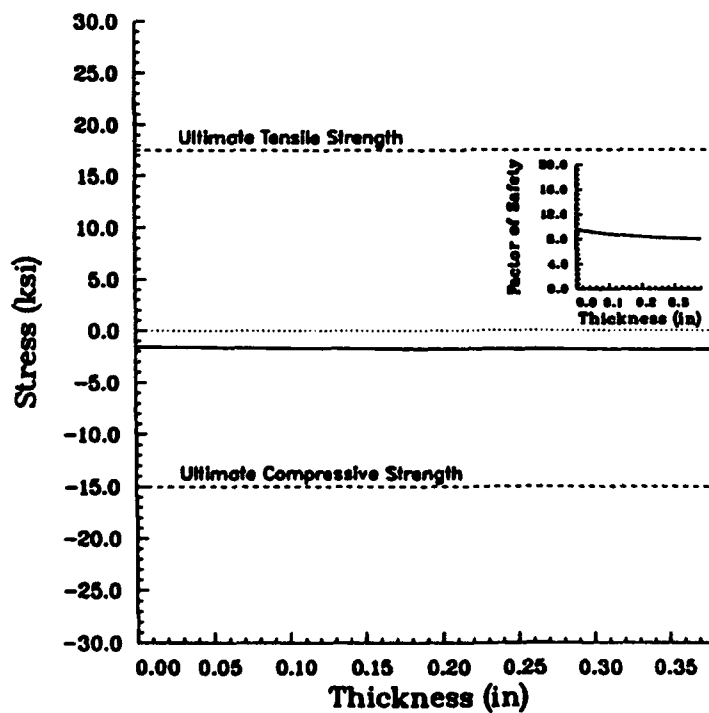


FIGURE C-10. FM16771-F BENDING STRESSES (X=13.875 IN.) VS. ABLATIVE THICKNESS

FIGURE C-11. FM16771-A BENDING STRESSES ($X=0$ IN.) VS. ABLATIVE THICKNESSFIGURE C-12. FM16771-A BENDING STRESSES ($X= 13.875$ IN.) VS. ABLATIVE THICKNESS

APPENDIX D
SHEAR STRESS IN ADHESIVE LAYER VS.
ABLATIVE ELASTIC MODULUS

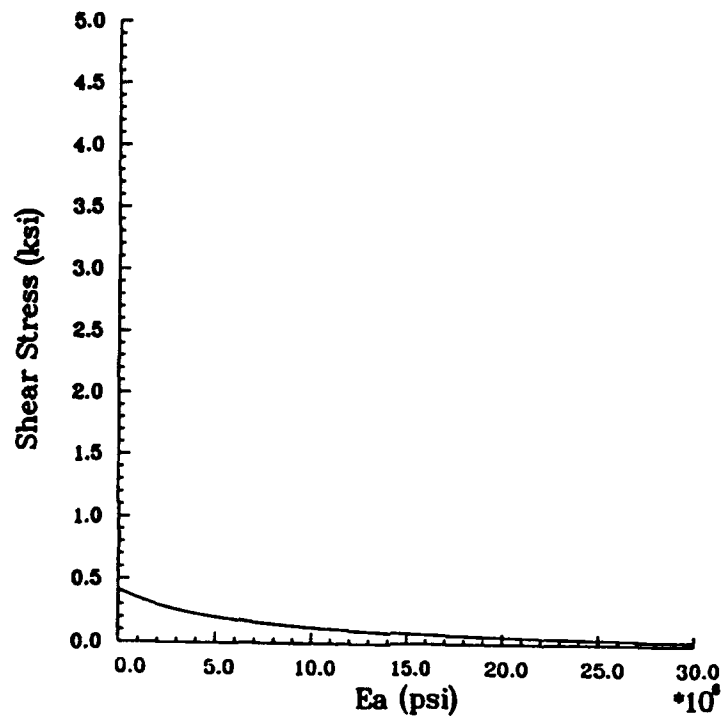


FIGURE D-1. ADHESIVE SHEAR STRESSES VS. ABLATIVE ELASTIC MODULUS
(HG=0.01 IN., EG=0.5 MSI)

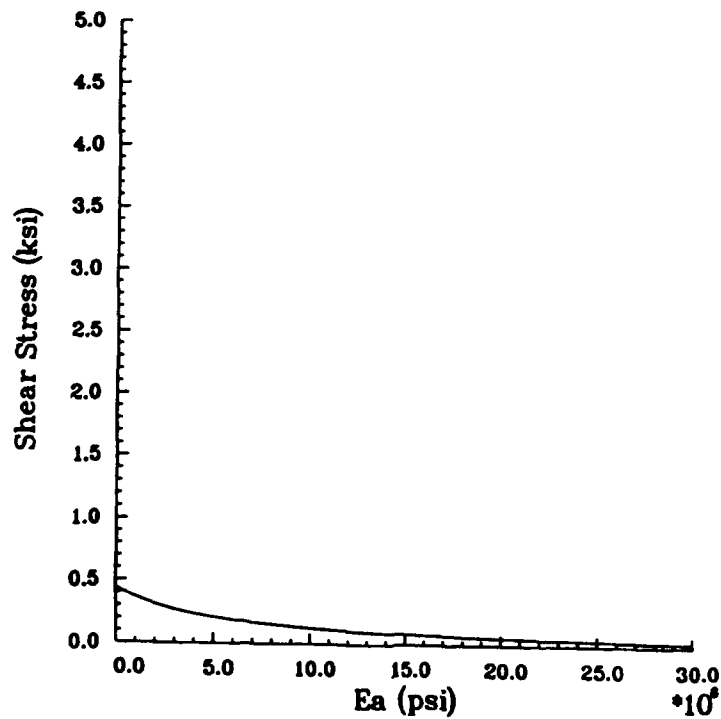


FIGURE D-2. ADHESIVE SHEAR STRESSES VS. ABLATIVE ELASTIC MODULUS
(HG=0.05 IN., EG=0.5 MSI)

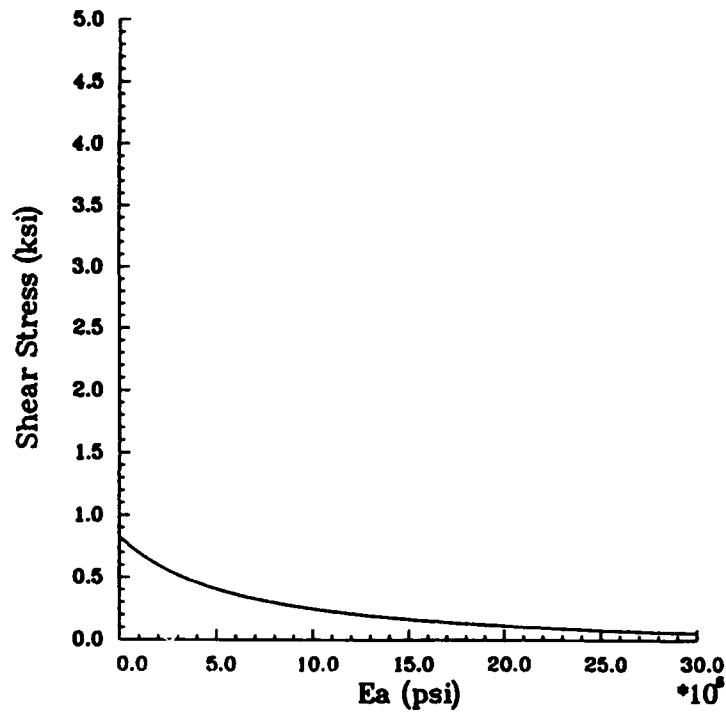


FIGURE D-3. ADHESIVE SHEAR STRESSES VS. ABLATIVE ELASTIC MODULUS
(HG=0.01 IN., EG=1.0 MSI)

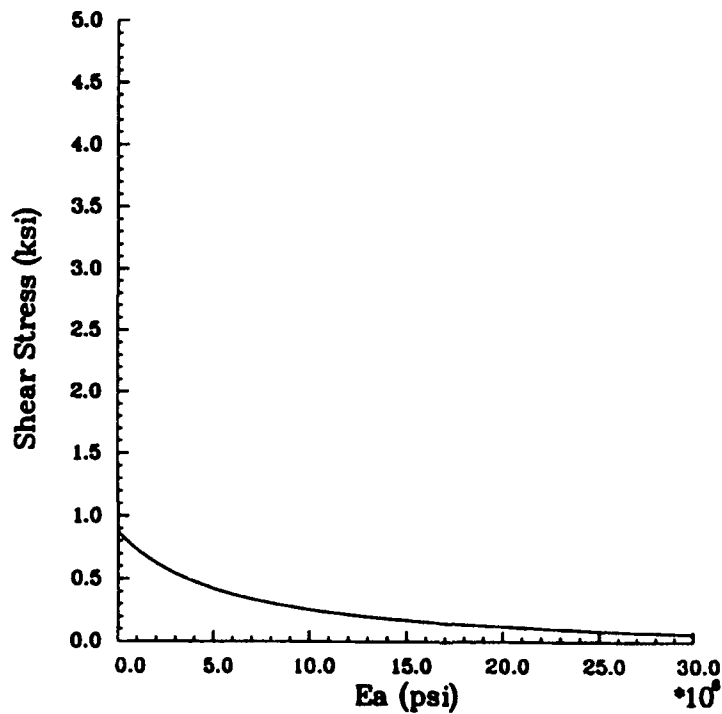


FIGURE D-4. ADHESIVE SHEAR STRESSES VS. ABLATIVE ELASTIC MODULUS
(HG=0.05 IN., EG=1.0 MSI)

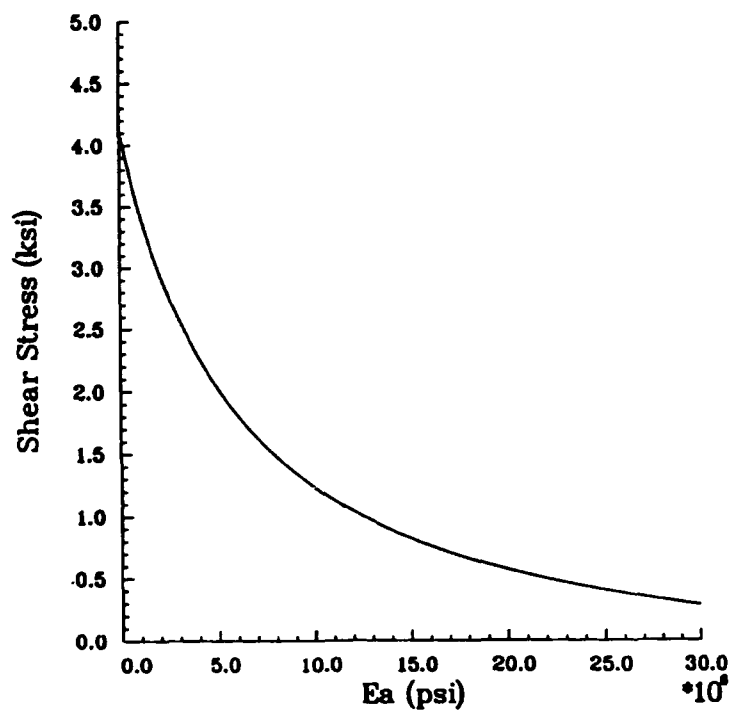


FIGURE D-5. ADHESIVE SHEAR STRESSES VS. ABLATIVE ELASTIC MODULUS
(HG=0.01 IN., EG=5.0 MSI)

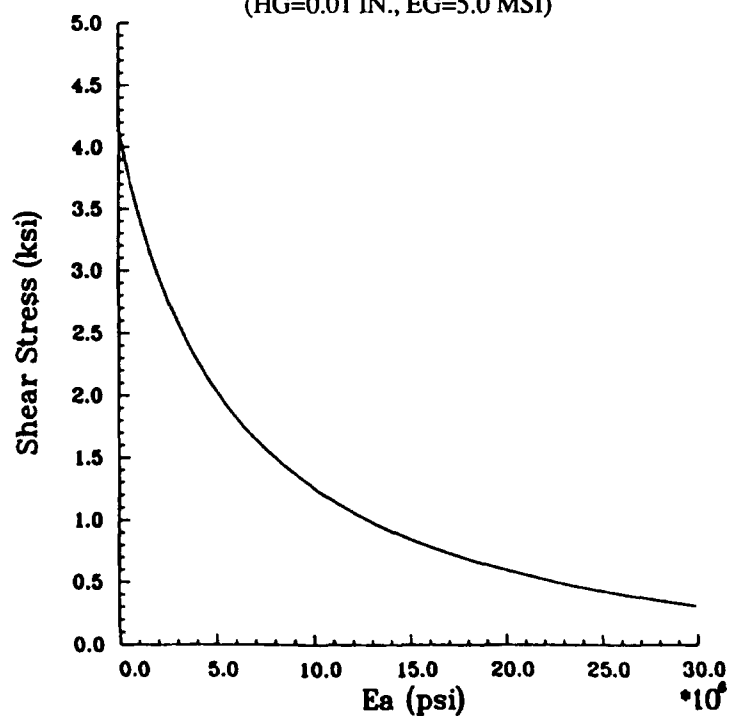


FIGURE D-6. ADHESIVE SHEAR STRESSES VS. ABLATIVE ELASTIC MODULUS
(HG=0.05 IN., EG=5.0 MSI)

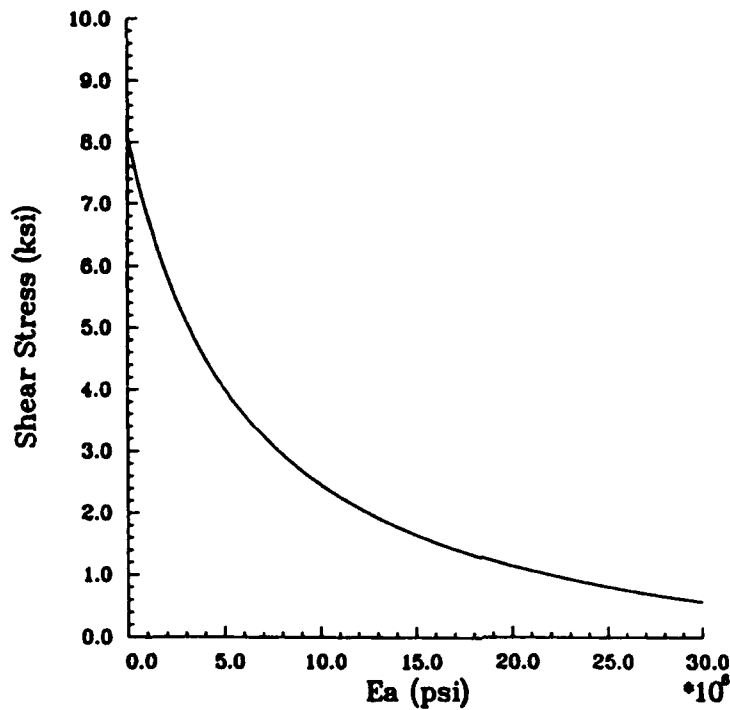


FIGURE D-7. ADHESIVE SHEAR STRESSES VS. ABLATIVE ELASTIC MODULUS
(HG=0.01 IN., EG=10.0 MSI)

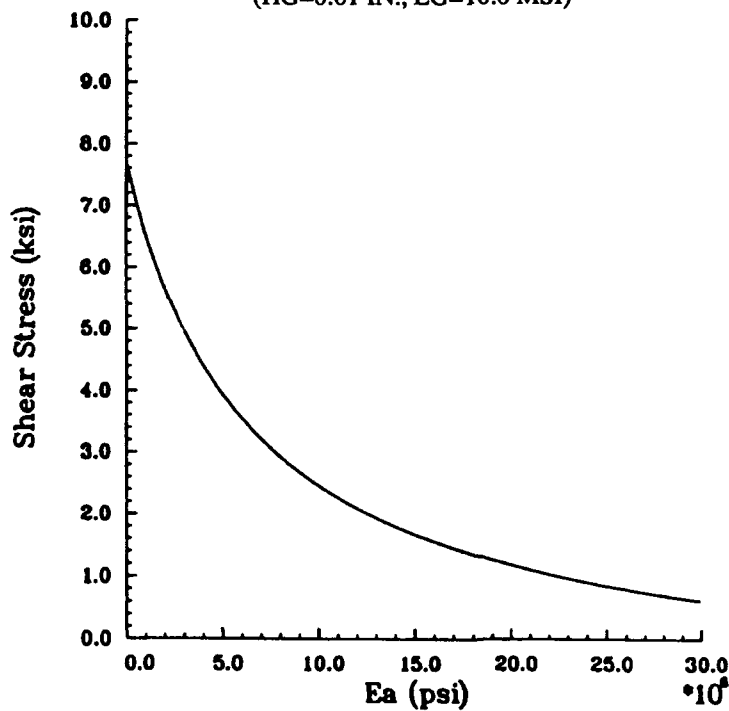


FIGURE D-8. ADHESIVE SHEAR STRESSES VS. ABLATIVE ELASTIC MODULUS
(HG=0.05 IN., EG=10.0A MSI)

DISTRIBUTION

	<u>COPIES</u>		<u>COPIES</u>
ATTN PMS4003B K PAYNE	1	ATTN AL PUHL	1
PMS420-11 M MILLER	1	NATHAN RUBINSTEIN	1
PMS422-11	1	JOHNS HOPKINS ROAD	
PMS422-12	1	APPLIED PHYSICS LABORATORY	
PMS422-31	1	LAUREL MD 20707	
062ZN1	1		
062ZN2	1	ATTN KENNETH A TAYLOR	1
COMMANDER		RAYTHEON COMPANY	
NAVAL SEA SYSTEMS COMMAND		EQUIPMENT DIVISION	
NAVAL SEA SYSTEMS COMMAND		430 BOSTON POST RD	
HEADQUARTERS		WAYLAND MA 01778	
2531 NATIONAL CITY BLDG 3			
WASHINGTON DC 20362-5160		ATTN JOSEPH H KOO	1
		MARK SCHNEIDER	1
ATTN CODE 3276 ALLEN GEHRIS	1	DAVID HEIM	1
COMMANDING OFFICER		WINSTON CHUCK	1
NAVAL AIR WEAPONS STATION		SHAN LIN	1
CHINA LAKE CA 93555-6001		MIKE MILLER	1
		MIKE KNEER	1
ATTN CODE 4L24 FORREST SICKLER	1	FMC CORPORATION	
COMMANDER		NAVAL SYSTEMS DIVISION	
PORT HUENEME DIVISION		4800 EAST RIVER RD	
NAVAL SURFACE WARFARE CENTER		PO BOX 59043	
PORT HUENEME CA 93043-5007		MINNEAPOLIS MN 55459-0043	
CENTER FOR NAVAL ANALYSES		ATTN CASS LAUX	1
4401 FORD AVE		DAVID ADAMS	1
ALEXANDRIA VA 22302-0268	1	MARTIN MARIETTA AERO AND	
		NAVAL SYSTEMS	
DEFENSE TECHNICAL INFORMATION		103 CHESAPEAKE PARK PLACE	
CENTER		BALTIMORE MD 21220	
CAMERON STATION			
ALEXANDRIA VA 22304-6145	12	ATTN JACK SIKONIA	1
		STEVE GONZY	1
ATTN GIFT AND EXCHANGE DIVISION	4	ALLIED SIGNAL RESEARCH AND	
LIBRARY OF CONGRESS		TECHNOLOGY	
WASHINGTON DC 20540		PO BOX 1021R	
		MORRISTOWN NJ 07962-1021	

DISTRIBUTION (Continued)

	<u>COPIES</u>		<u>COPIES</u>
ATTN HAL WEATHERLY	1	ATTN CLINT JUHL	1
AMERICAN POLYTHERM CO INC		RAY WILLIAMS	1
2000 FLIGHTLINE DR		ICI FIBERITE	
LINCOLN CA 95648		23271 VERDUGO DR	
		SUITE A	
ATTN BERT HECHT	1	LAGUNA HILLS CA 92653	
ARCADY CHECHIK	1		
AMETEK INC		ATTN BILL GRAHAM	1
HAVEG DIVISION		GERHARD SCHIROKY	1
900 GREENBANK RD		LANXIDE CORP	
WILMINGTON DE 19808		1300 MARROWS RD	
		PO BOX 6077	
ATTN FRED SEIBERT	1	NEWARK DE 19714-6077	
DON BECKLEY	1		
BP CHEMICALS (HITCO) INC		ATTN JIM WHITE	1
700 E DYER RD		SWEDLOW INC	
SANTA ANA CA 92705-5611		12122 WESTERN AVE	
		GARDEN GROVE CA 92645	
ATTN CHIP ROTH	1		
JERRY HARTMAN	1	ATTN WILHELM BETZ	1
HERMANT GUPTA	1	BRANDENBERGER	
SP SYSTEMS		ISOLIERTECHNIK GMBH & CO KG	
MONTECATINI ADVANCED MATERIALS		POSTFACH 1164 + 1165	
5915 RODEO RD		TAUBENSUHLSTRASSE 6	
LOS ANGELES CA 90016		D-6470 LANDAU/PFALZ	
		WEST GERMANY	
ATTN SCOTT STEPHENSON	1		
FIBER MATERIALS INC		ATTN KLAUS MEYER	1
5 MORIN ST		FRATHERM ISOLIERUNGS GMBH	
BIDDEFORD INDUSTRIAL PK		POSTFACH 90 93 69	
BIDDEFORD ME 04005-4497		FRAUENLOBSTRASSE 2	
		D-6000 FRANKFURT/MAIN 90	
ATTN ED HEMMELMAN	1	WEST GERMANY	
DAN DALENBERG	1		
ICI FIBERITE		ATTN DANIEL QUENTIN	1
501 WEST THIRD ST		SNPE	
WINONA MN 55987		US OPERATIONS	
		1111 JEFFERSON DAVIS HWY	
		SUITE 700	
		ARLINGTON VA 22202	

DISTRIBUTION (Continued)

	<u>COPIES</u>		<u>COPIES</u>
ATTN JACKY PATTEIN	1	H13	1
SNPE		H13 ANDERSON	1
ARMOR COMPOSITES		H13 BOYER	1
29590 POINT DE BUIS		H13 CHESTER	1
FRANCE		H13 DELOACH	1
		H13 POWERS	25
ATTN ETIENNE SUBRENAT	1	H13 SOO HOO	1
SEP		K205 MESSICK	1
SOLID PROPULSION AND		K22 OPEKA	1
COMPOSITES DIV		K22 VARICK	1
LE HAILLAN BP 37		N74 GIDEP	1
33165 SAINT MEDARD EN JALLES		R31	1
FRANCE		R31 DUFFY	1
		R31 HAUGHT	1
ATTN CLAUDE BONNET	1	R31 TALMY	1
SEP INC		R31 WELLER	1
1100 17TH ST NW		R31 ZAYKOSKI	1
SUITE 320		R34 LIU	1
WASHINGTON DC 20036		R34D	1
TPRL			
CINOAS BUILDING			
2595 YEAGER RD			
WEST LAFAYETTE IN 47906	1		
INTERNAL DISTRIBUTION:			
E231	3		
E232	2		
E281 FINK	1		
D4	1		
G205	1		
G21	1		
G21 ATKINSON	1		
G21 MILLS	1		
G21 PRITCHETT	1		
H02	1		
H023	1		
H10	1		
H11 BOWEN	1		
H11 GESSLER	1		

REPORT DOCUMENTATION PAGE			Form Approved OBM No. 0704-0188	
Public reporting burden for this collection of information is estimated to average 1 hour per response, including the time for reviewing instructions, searching existing data sources, gathering and maintaining the data needed, and completing and reviewing the collection of information. Send comments regarding this burden or any other aspect of this collection of information, including suggestions for reducing this burden, to Washington Headquarters Services, Directorate for Information Operations and Reports, 1215 Jefferson Davis Highway, Suite 1204, Arlington, VA 22202-4302, and to the Office of Management and Budget, Paperwork Reduction Project (0704-0188), Washington, DC 20503.				
1. AGENCY USE ONLY (Leave blank)		2. REPORT DATE October 1992		3. REPORT TYPE AND DATES COVERED
4. TITLE AND SUBTITLE Structural Performance of Candidate Ablatives for Uptake Section of Vertical Launching System			5. FUNDING NUMBERS	
6. AUTHOR(S) John Powers				
7. PERFORMING ORGANIZATION NAME(S) AND ADDRESS(ES) Naval Surface Warfare Center Dahlgren Division (H13) Dahlgren, Virginia 22448-5000			8. PERFORMING ORGANIZATION REPORT NUMBER NSWCDD/TR-92/477	
9. SPONSORING/MONITORING AGENCY NAME(S) AND ADDRESS(ES)			10. SPONSORING/MONITORING AGENCY REPORT NUMBER	
11. SUPPLEMENTARY NOTES				
12a. DISTRIBUTION/AVAILABILITY STATEMENT Authorized for public release; distribution is unlimited.			12b. DISTRIBUTION CODE	
13. ABSTRACT (Maximum 200 words) The structural performance of several candidate ablatives for the uptake section of the Navy's Vertical Launching System is investigated. The uptake is modeled using a fixed-fixed beam loaded by a uniform pressure. Beam displacement field equations are solved, assuming that the ablatives exhibit bimodular behavior in tension and compression. The candidate ablatives are ranked according to predicted structural performance. The current uptake ablative, MXBE-350, possesses the highest factor of safety in this analysis, although all but one of the ablatives considered appears to be acceptable. Additionally, the effects of erosion on the magnitudes of the peak stresses seen by the virgin ablatives are analyzed by varying the thickness of the ablatives in the uptake. As the thickness of the ablative decreases, the peak stresses in the ablative decrease. Finally, the effect of the stiffness of the ablative on predicted stresses in the adhesive layer is computed. As the elastic modulus of the ablative increases, the stresses in the adhesive decrease.				
14. SUBJECT TERMS Vertical Launching System Uptake, Structural Performance of Ablatives, Ablatives			15. NUMBER OF PAGES 87	
			16. PRICE CODE	
17. SECURITY CLASSIFICATION OF REPORT UNCLASSIFIED	18. SECURITY CLASSIFICATION OF THIS PAGE UNCLASSIFIED	19. SECURITY CLASSIFICATION OF ABSTRACT UNCLASSIFIED	20. LIMITATION OF ABSTRACT SAR	